































RESEARCH ARTICLE

Comprehensive phylogenomic time tree of bryophytes reveals deep relationships and uncovers gene incongruences in the last 500 million years of diversification

Julia Bechteler^{1,2}  | Gabriel Peñaloza-Bojacá³  | David Bell⁴  |
 J. Gordon Burleigh⁵  | Stuart F. McDaniel⁵  | E. Christine Davis⁵ |
 Emily B. Sessa⁵  | Alexander Bippus⁶  | D. Christine Cargill⁷  |
 Sahut Chantanoarrapint⁸  | Isabel Draper⁹  | Lorena Endara⁵  |
 Laura L. Forrest⁴  | Ricardo Garilleti¹⁰  | Sean W. Graham¹¹  |
 Sanna Huttunen¹²  | Javier Jauregui Lazo¹³  | Francisco Lara⁹  |
 Juan Larraín¹⁴  | Lily R. Lewis⁵  | David G. Long⁴  | Dietmar Quandt¹  |
 Karen Renzaglia¹⁵  | Alfons Schäfer-Verwimp¹⁶  | Gaik Ee Lee¹⁷  |
 Adriel M. Sierra¹⁸  | Matt von Konrat¹⁹  | Charles E. Zartman²⁰  |
 Marta Regina Pereira²¹  | Bernard Goffinet²²  | Juan Carlos Villarreal A.¹⁸ 

Correspondence

Juan Carlos Villarreal A., Département de Biologie, Université Laval, Québec, Québec G1V 0A6, Canada.
 Email: juan-carlos.villarreal-aguilar@bio.ulaval.ca

Bernard Goffinet, Ecology and Evolutionary Biology, University of Connecticut, 75 North Eagleville Road, Storrs, VT 06269-3043 USA.
 Email: bernard.goffinet@uconn.edu

Present addresses

Emily B. Sessa, The New York Botanical Garden, 2900 Southern Boulevard, Bronx, NY 10458, USA.

Lorena Endara, Department of Biological Sciences, Clemson University, 132 Long Hall, Clemson, SC 29634, USA.

Abstract

Premise: Bryophytes form a major component of terrestrial plant biomass, structuring ecological communities in all biomes. Our understanding of the evolutionary history of hornworts, liverworts, and mosses has been significantly reshaped by inferences from molecular data, which have highlighted extensive homoplasy in various traits and repeated bursts of diversification. However, the timing of key events in the phylogeny, patterns, and processes of diversification across bryophytes remain unclear.

Methods: Using the GoFlag probe set, we sequenced 405 exons representing 228 nuclear genes for 531 species from 52 of the 54 orders of bryophytes. We inferred the species phylogeny from gene tree analyses using concatenated and coalescence approaches, assessed gene conflict, and estimated the timing of divergences based on 29 fossil calibrations.

Results: The phylogeny resolves many relationships across the bryophytes, enabling us to resurrect five liverwort orders and recognize three more and propose 10 new orders of mosses. Most orders originated in the Jurassic and diversified in the Cretaceous or later. The phylogenomic data also highlight topological conflict in parts of the tree, suggesting complex processes of diversification that cannot be adequately captured in a single gene-tree topology.

Conclusions: We sampled hundreds of loci across a broad phylogenetic spectrum spanning at least 450 Ma of evolution; these data resolved many of the critical nodes of the diversification of bryophytes. The data also highlight the need to explore the mechanisms underlying the phylogenetic ambiguity at specific nodes. The phylogenomic

For affiliations refer to page 15.

Julia Bechteler, Gabriel Peñaloza-Bojacá, J. Gordon Burleigh, Bernard Goffinet, and Juan Carlos Villarreal A. contributed equally to this article.

This is an open access article under the terms of the Creative Commons Attribution-NonCommercial-NoDerivs License, which permits use and distribution in any medium, provided the original work is properly cited, the use is non-commercial and no modifications or adaptations are made.

© 2023 The Authors. *American Journal of Botany* published by Wiley Periodicals LLC on behalf of Botanical Society of America.

data provide an expandable framework toward reconstructing a comprehensive phylogeny of this important group of plants.

KEYWORDS

Cretaceous diversification, hornworts, land plants, liverworts, mosses, phylogenetic discordance, rapid diversification, target capture

Recent findings that the haploid-dominant bryophytes, i.e., the hornworts, liverworts, and mosses (Figure 1), form a clade sister to the diploid-dominant vascular plants (Puttick et al., 2018; Sousa et al., 2019) have made inferences about the morphological elaboration of land-plant gametophytes and sporophytes more uncertain than previous inferences that placed vascular plants in a more nested position (Rich and Delaux, 2020). Key elements of land plant development, including meristem function (Cammarata et al., 2022), stomatal development (Harris et al., 2020), and hormone responses (Bennett et al., 2014; Lavy et al., 2016), are built from a conserved genomic blueprint (Harris et al., 2020). From a sporophyte perspective, bryophyte genomes hold signatures of divergence and reduction from a morphologically complex ancestor (Harris et al., 2022). Yet our understanding of the genomic basis of gametophytic evolution across land plants is comparatively less well understood. Bryophytes are important components of various ecological communities and contribute to local nutrient fluxes and global biogeochemical cycles (Porada et al., 2013, 2014; Stuart et al., 2021; Eldridge et al., 2023). Broad evolutionary analyses are key for assessing the significance of gametophyte trait variation in these roles. Reconstructing the history of bryophytes is therefore critical for understanding the transformations of developmental, physiological, and functional morphological traits across land plants (e.g., Puttick et al., 2018; Liu et al., 2019; Harris et al., 2022; Patiño et al., 2022).

The most recent common ancestor of bryophytes likely occurred approximately 480 million years ago (Ma) (Harris et al., 2022). The ages of many major morphologically defined bryophyte orders, however, remain less certain. Indeed, prior reconstructions lacked strong support at the ordinal level, either because the data included relatively few loci across many species or many genes across relatively few bryophyte taxa (Villarreal and Renner, 2012; Feldberg et al., 2014; Laenen et al., 2014; Morris et al., 2018; Harris et al., 2022). Furthermore, bryophyte fossils are few and mostly from the Cretaceous or younger sediments, and the affinities of older fossils to lineages defined by extant taxa have only recently been reassessed in light of new systematic and phylogenetic hypotheses (Tomescu et al., 2018; Feldberg et al., 2021; Ignatov and Maslova, 2021; Bippus et al., 2022).

To infer a comprehensive bryophyte phylogeny, we collected sequence data from 405 exons within 228 nuclear genes using the GoFlag 408 flagellate land plant probe set for 531 species sampled from virtually all orders. Although these data provided strong support for many clades in the phylogeny, they also highlight areas of gene-tree

discordance that were largely unrecognized in previous phylogenetic analyses of primarily organellar sequence data. Based on our analyses, we propose to resurrect five liverwort orders and to recognize three new liverwort and 10 new moss orders. We also estimated divergence times and absolute rates of molecular evolution based on the most recent assessments of the affinities of liverwort (Feldberg et al., 2021) and moss (Ignatov and Maslova, 2021) fossils. Collectively, these analyses provide the basis to further dissect diversification processes at multiple phylogenetic scales across the bryophytes (Breinholt et al., 2021).

MATERIALS AND METHODS

Taxon sampling

We sampled 531 bryophyte species belonging to 499 genera distributed among 72% of families from 52 of the 54 orders of bryophytes (i.e., all except the moss orders Pseudoditrichales and Bryoxiphiales; Appendix S1, Table S1). The 362 moss species represent 338 genera (34% of all genera), the 159 liverwort species represent 151 genera (37% of all genera), and 12 hornwort species from all 10 genera. Sequences from 41 of these samples were previously published (Breinholt et al., 2021; Draper et al., 2022; Jauregui-Lazo et al., 2023), and those obtained for the remaining 490 samples are new to this study (Appendix S1, Table S1). Taxon sampling percentage values were calculated using recent checklists and classification literature (Söderström et al., 2016; Brinda and Atwood, 2023). The trees are rooted with the hornworts, assumed to be the sister group of the setaphytes (Renzaglia et al., 2018), i.e., liverworts and mosses (Leebens-Mack et al., 2019).

DNA extraction

We used the modified cetyltrimethylammonium bromide (CTAB) extraction protocol (Doyle and Doyle, 1987) described by Breinholt et al. (2021) for most of the samples. This protocol includes lysing the cells by centrifuging them and washing with two rounds of 24:1 v/v chloroform–isoamyl alcohol, followed by cold isopropanol precipitation and a 70% v/v ethanol wash. We added 2 μ L of 10 mg/mL RNase A (QIAGEN, Valencia, CA, USA) to remove RNA contamination between chloroform washes. For a few specimens (i.e., Lejeuneaceae), we used the Invisorb Spin Plant Mini Kit (Strattec Molecular GmbH, Berlin, Germany).



FIGURE 1 Representatives of major lineages of bryophytes and examples of traits unique to hornworts, liverworts, and mosses. (A) Hornwort with longitudinally dehiscing sporophyte: *Anthoceros nesii*. (B) Pyrenoid (arrowheads) of the hornwort *Phaeoceros perpusillus*. (C) Complex thalloid liverwort: *Marchantia paleacea*. (D) Simple thalloid liverwort: *Metzgeria conjugata*. (E) Leafy liverwort: *Leiocolea badensis*. (F) Liverwort sporophyte before (left) and after (right) dehiscence: *Fossombronia pusilla*. (G) Oil bodies of *Gymnocolea inflata*. (H) Polytrichopsida moss: *Atrichopsis trichodon*. (I) Acrocarpous moss: *Orthotrichum anomalum*. (J) Pleurocarpous moss: *Exsertotheca intermedia*. (K) Nematodontous peristome of *Polytrichum ohioense*. (L) Arthrodontous peristome of *Bryum capillare*. Pictures kindly shared by Štěpán Koval (A, D, E, F, I), Sahut Chantanaorrapint (B), Des Callaghan (C, J, L), Bernard Goffinet (H), Jerry Jenkins (K), and David Wagner (G).

TARGET ENRICHMENT AND SEQUENCING ASSEMBLY

We generated a multilocus nuclear sequence data set with a target enrichment approach using the GoFlag flagellate land plant probe sets. We assembled published data from 41 samples generated using the GoFlag 451 flagellate land plant probe set (Breinholt et al., 2021). The sequence data from the remaining 490 samples were generated using the GoFlag 408 flagellate land plant probe set, which is an optimized subset of the GoFlag 451 probe set consisting of 53,306 probes covering 408 exons

from single- or low-copy nuclear loci. The library preparation, target enrichment, and sequencing were done by RAPiD Genomics (Gainesville, FL, USA) using protocols described by Breinholt et al. (2021), with the enriched, pooled libraries sequenced on an Illumina HiSeq 3,000 platform (Illumina, San Diego, CA, USA; 2 × 100 bp). The paired-end raw reads are available in the NCBI SRA database (Appendix S1, Table S1).

We assembled phylogenetic sequence alignments for each locus using the iterative baited assembly “pipeline” (i.e., a series of scripts and commands designed to link the output of one step to the input of the next; Breinholt et al., 2021).

In some loci, the pipeline retains more than one copy per sample where the Bridger assembler (Chang et al., 2015) interprets greater than simple allelic variation. In some cases, these also may represent contaminant sequences from mixed samples, which occasionally occur in bryophyte specimens. To minimize the inclusion of possible paralogs or contaminants, we removed all copies of a sample in a locus alignment. Next, we removed any columns in the alignments that had nucleotide data from fewer than 10 samples in all output files (PHYLIP format). We also pruned out potentially anomalous sequences associated with excessively long branches in the locus trees. To remove the sequences associated with excessively long branches, we first, inferred maximum likelihood (ML) trees from the locus alignments using RAxML and the GTR CAT model, and we rooted the resulting gene trees with Newick Utilities (Junier and Zdobnov, 2010) using the hornworts as the outgroup. We eliminated one locus for which hornworts were not monophyletic. For the others, we calculated the root to tip distance for each taxon and pruned out any sequences that had a root to distance >3 standard deviations more than the average distance for sequences from that locus, thus removing 750 of 178,650 sequences. We then further examined the branches with lengths >1 by eye and removed 35 additional long-branch sequences that appeared anomalous.

All loci in the GoFlag probe sets correspond to nuclear exons, some of which are part of the same gene (see Appendix S3 from Breinholt et al., 2021, which maps the GoFlag loci to their respective “single copy” 1KP gene). After our screening, we were left with alignments from 405 of the 408 loci (i.e., exons) covered by the GoFlag flagellate land plant probe set. We concatenated the loci found in the same gene, resulting in 228 alignments, each containing between one and nine exons. These gene alignments were used to build “gene” trees. Combining loci from the same gene implicitly assumes that there is no recombination within the gene, but a longer gene alignment may reduce stochastic error in gene-tree inference. The average length of the 228 alignments was 339.7 bp (min = 120, max = 1459), with a mean of 238.4 of potentially parsimony informative sites per alignment (min = 66, max = 1065) and a low average percentage of missing data (8.61%, min = 0.000%, max = 43.72%; Appendix S1, Table S2).

We also created amino acid alignments for each locus by taking the original locus nucleotide alignments and removing any columns in the sequence alignments with only one nucleotide, which most likely represented sequencing error. We then used AliView (Larsson, 2014) to make edits by hand to put the alignments in frame, which usually requires minimal editing. We then saved the corresponding amino acid alignments and again concatenated the loci from the same gene before making gene trees. To make the concatenated supermatrices for ML analysis, we concatenated all the locus alignments for the nucleotides and then also for the amino acids.

Species tree analyses

We conducted species tree analyses for the nucleotide and the amino-acid gene trees using ASTRAL-III v.5.7.7 (Zhang et al., 2018). We inferred gene trees from the nucleotide alignments with RAxMLv.8.2.9 (Stamatakis, 2006, 2014) using the default RAxML tree search algorithm (-f d) and the GTR+GAMMA nucleotide substitution model. For the amino acid alignments, we inferred gene trees with IQ-TREE v.2.1 using the substitution model chosen automatically based on model testing. In the ASTRAL-III analyses, we used the default settings and computed the local posterior probabilities (Sayyari and Mirarab, 2016) and quartet scores for all three resolutions per branch (-t 8). The resulting ASTRAL topologies were annotated with quartet support values for the main topology (q1), the first alternative topology (q2), and the second alternative topology (q3) (Sayyari and Mirarab, 2016).

ML concatenated supermatrix and gene concordance analyses

We performed ML phylogenetic inferences with 100 replicates of rapid bootstrapping on the concatenated nucleotide data set using IQ-TREE v.2.1 (Nguyen et al., 2015) with the GTRGAMMA model of sequence evolution. For the amino acid data set, we used IQ-TREE v.2.1 and performed auto model selection (ModelFinder) and tree inference separately for each gene. Branch support for the amino acid data set was assessed using 1000 replicates of ultrafast bootstrapping (Hoang et al., 2017).

To investigate topological conflict around each branch of the species tree for the nucleotide and amino acid data sets, we estimated the gene (gCF) and site (sCF) concordance factors in IQ-TREE, using the “-gcf and -scf” options (Minh et al., 2020). Likewise, we compared the species and gene trees generated with ASTRAL and IQ-TREE (maximum likelihood) to assess and evaluate gene tree–species tree incongruence. For these analyses, we focused on 111 backbone nodes (labelled in Figure 2) of the ASTRAL tree using the quartet values from the ASTRAL analyses (Appendix S1, Table S3–S7).

Concordance analyses were calculated for every branch of the species tree; the gCF and sCF represent the percentage of decisive genes and sites, respectively. IQ-TREE also estimates gDFP (gene discordant factor due to paraphyly) or the gene discordance factor due to lack of information in the genes or paraphyly of the quartet. For measures of support, gene concordance factor and site concordance factor (gCF/sCF) were categorized as follows: weak <33%, moderate 33–50%, strong >50% (following Minh et al., 2020; Cooper et al., 2022). Using the ASTRAL output, we performed exploratory analyses to assess whether patterns of gene tree are consistent with the neutral ILS (incomplete lineage sorting) model using IQ-TREE. To estimate ILS, we performed χ^2 tests to

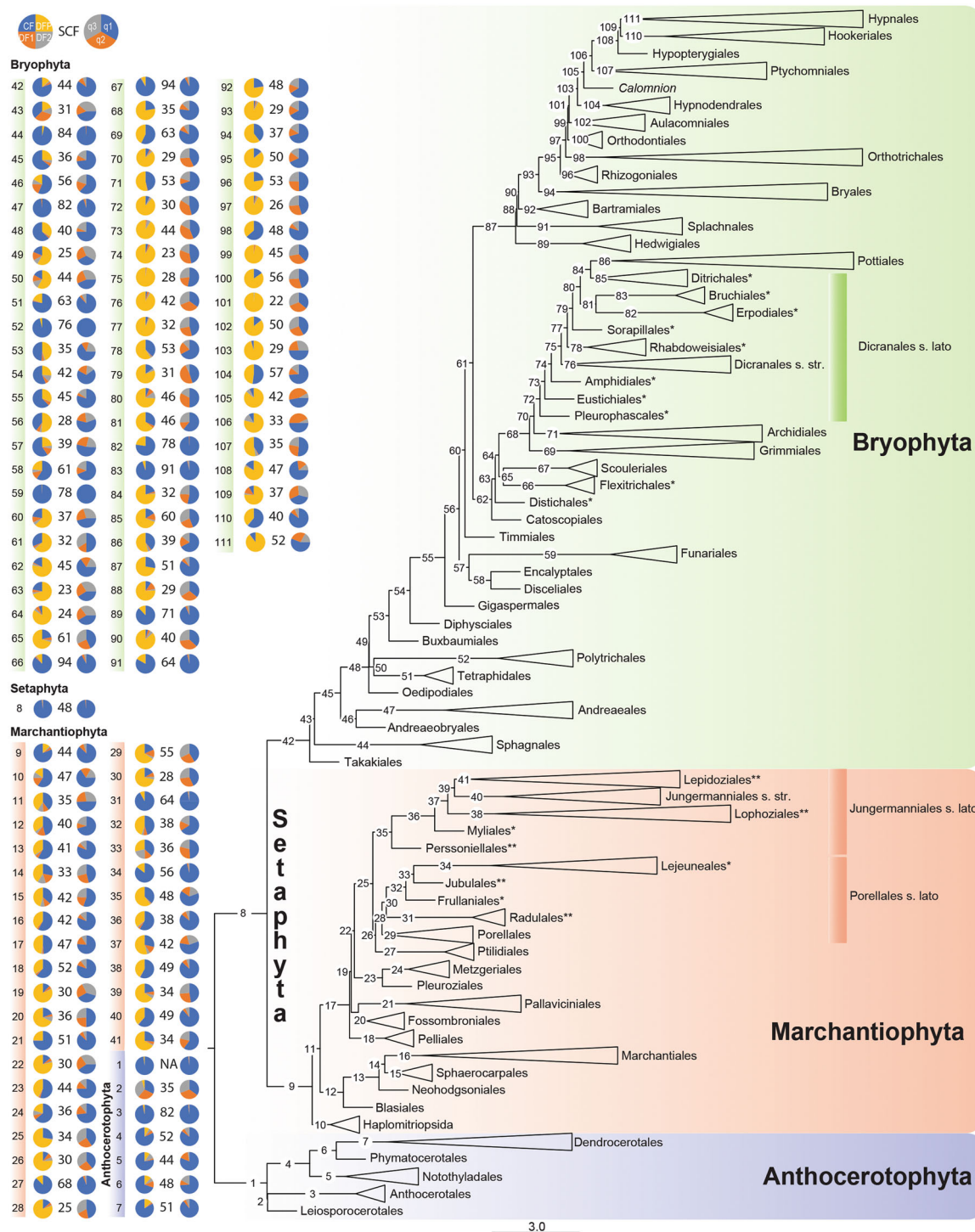


FIGURE 2 Phylogenetic inferences for 531 species from 499 genera belonging to orders from all three bryophyte groups (mosses, liverworts, and hornworts) based on ASTRAL analysis of 228 nuclear gene trees (Appendix S1, Tables S1 and S3). The phylogram shows internal branch lengths relative to coalescent units between branching events, as estimated by ASTRAL-III v.5.7.7. The nodes of interest (highlighted by major clade color) have been numbered to illustrate quartet values from gene concordance factor (gcf) values (left), while the number in the center is the site concordance factor (sCF). gCF and sCF represent the percentage of decisive genes and sites at each branch, respectively. Pies for quartet values from concordance factor values: CF (topology shown) and alternative options (DF1, DF2, DFP); see Appendix S1 (Tables S4–S6) for the concordance factors for all nodes. Quartet values from ASTRAL analyses presented as pie charts (right). ASTRAL pies are divided into q1 or topology shown (blue), q2 (orange, 2nd alternative hypothesis) and q3 (grey, 3rd alternative hypothesis) with the percentage for q1 included in the pie diagram; see Figures S1, S2 for quartet values for all other nodes and local posterior probabilities. *Newly proposed order; **resurrected order. Scale bar: 3 coalescent units.

determine whether we can reject the hypothesis that the number of trees or sites supporting discordant topologies with roughly equal quartet values. Under the assumption of ILS, the discordant topologies should be supported by an approximately equal number of gene trees or sites (Appendix S1, Tables S4, S7), which would result in a nonsignificant χ^2 . Rejecting the null hypothesis suggests that processes other than ILS, including possibly gene tree error, may be contributing to the discordance. Additionally, equal quartets, gcf or scf (~33%) for the tree quartets may also suggest ILS (Minh et al., 2020). Successive rapid diversification coupled with ILS could contribute to a number of conflicting topologies.

Divergence time estimation

Divergence time was estimated using treePL (Smith and O'Meara, 2012) and the analysis guidelines of Maurin (2020). We selected the best-ML tree from the nucleotide concatenated analysis as input for treePL (see above). To infer confidence intervals on the dated tree, we ran 1000 bootstrap replicates through the “Bootstrap+Consensus” workflow of RAxML-HPC2 on XSEDE on the CIPRES Science Gateway (Miller et al., 2011) using the best ML tree as constraint, partitioning scheme by genes, and using the GTR+GAMMA substitution model. All trees were rooted with hornworts as the sister group of other bryophytes using the program pxrr in phyx (Brown et al., 2017).

We took advantage of the recent comprehensive reviews of the liverwort and moss fossil records (Feldberg et al., 2021; Ignatov and Maslova, 2021) to calibrate 16 liverwort and 13 moss nodes (Appendix S1, Table S8) and implemented a maximum age constraint of the root of 515 Ma (Morris et al., 2018). Priming and cross-validation analyses were performed using the best-ML tree and all 29 calibrations. Best optimization parameters were implemented as follows: opt = 2, optad = 2, optcvad = 5. Cross-validation used these parameters and repeated four times, reaching a stable smoothing parameter = 10. To obtain confidence intervals on the dated tree, we ran the treePL analysis with the bootstrap replicates using the same calibration, optimization, and cross-validation values as outlined above. The set of trees was summarized in TreeAnnotator v.2.6.6 (part of the BEAST package; Bouckaert et al., 2014) with mean node heights and 10% of burn in. Trees were visualized in FigTree v.1.4.3 (Rambaut, 2017). Lineage-through-time plots were constructed based on the treePL chronogram for all bryophyte taxa together, as well as liverworts and mosses separated using the R package ape (Paradis and Schliep, 2019; R Core Team, 2020). We visualized the temporal distribution of order and family ages using the average stem and crown age. Monotypic families and orders were excluded from the calculations (Appendix S1, Table S9). Bryophyte species numbers were obtained from Söderström et al. (2016) and Brinda and Atwood (2023).

Absolute rates of molecular evolution were estimated with the same calibrations and targeted ML trees using r8s (Sanderson, 2003) (Appendix S1, Table S10).

RESULTS AND DISCUSSION

Coalescent-based (ASTRAL) and maximum likelihood (ML) concatenated super-matrix analyses (RAxML, IQ-TREE) of nucleotide and amino acid data yielded similar trees (Figure 2; Appendix S2–S7). In the following sections, we present the results from the ASTRAL analyses of gene trees inferred from nucleotide and amino acid data, including quartet values and gene concordance factors (gCF) and site concordance factors (sCF). We refer to a majority of gene trees when more than 50% of these share a given signal, and a plurality of gene trees when the proportion of trees supporting the topology is higher than 33% but less than 50%. However, support from a majority or plurality of gene-trees at a node does not necessarily reflect the level of gene tree discordance. The gene trees that do not support the node may conflict with the species tree topology, or they may be non-informative regarding the species tree node. ASTRAL quartet values and IQ-TREE concordance factors for nucleotide and amino acid analyses are presented in Appendix S1–S12 and the supplementary figures are available in the Dryad repository (<https://doi.org/10.5061/dryad.3j9kd51qm>; Bechteler et al., 2023).

Current classifications of bryophytes follow a Linnean scheme, a strictly hierarchical organization, with taxa at one rank nested within the taxon of the next higher rank (e.g., Renzaglia et al. [2009] for hornworts; Crandall-Stotler et al. [2009a, b] for liverworts; Goffinet et al. [2009a, b] for mosses). Each taxon is defined by one or more diagnostic traits. Historically, variation in morphological and developmental traits provided the basis for classifying organisms into taxa. For a review of systematic concepts of lineages of hornworts, see Hässel de Menéndez [1988], Schuster [1992], Stotler and Crandall-Stotler [2005], and Duff et al. [2007]; of liverworts, see Schuster [1984], and Crandall-Stotler and Stotler [2000]; and of mosses, see Crosby [1980] and Vitt [1984]). The underlying systematic concepts implicitly assume homology of putative diagnostic traits across members of a taxon. Reconstructions of phylogenetic relationships based on molecular or morphological traits, revealed, however, recurring homoplasy among traits and across the history of diversification of hornworts (e.g., Hyvönen and Piippo, 1993; Duff et al., 2004), liverworts (e.g., Davis, 2004; He-Nygrén et al., 2004; Crandall-Stotler et al., 2005; Forrest et al., 2006), and mosses (e.g., Goffinet et al., 1998; Hedderson et al., 1999; La Farge et al., 2000), prompting the revisions of concepts and hence classifications (e.g., Goffinet and Buck, 2004; Frey and Stech, 2005; Heinrichs et al., 2005; Duff et al., 2007; Stech and Frey, 2008). Homoplasy in morphological traits may obscure deep phylogenetic divergences and result in phenotypic similarity that may be perceived or interpreted as indicative of a more recent ancestry. For example, one of

the earliest molecular phylogenetic inferences highlighted that the monospecific moss genus *Oedipodium*, which lacks a peristome, was more closely related to the Polytrichales (nodes 50 and 52 in Figure 2) than to the vegetatively similar Splachnaceae (Vitt, 1984; node 91 in Figure 2).

Here we propose the recognition of new orders or ordinal circumscriptions within the liverworts and mosses (see Table 1 and taxonomic treatment below). In the latter, our proposals address primarily the extensive and recurrent recovery of a paraphyletic Dicranales, including the resolution of the Archidiales between the Micromitriaceae and Leucobryaceae, two families formerly included in the Dicranales (Goffinet et al., 2009b). The Dicranales have traditionally been rather broadly defined (Vitt, 1982), accommodating all families that lacked the diagnostic traits of the Grimmiaceae and Pottiales; hence, it is not surprising that the Dicranales have never been recovered as monophyletic based on inferences from DNA sequences (La Farge et al., 2000; Goffinet et al., 2001; Cox et al., 2010; Stech

et al., 2012; Fedosov et al., 2016, 2021, 2023; Bonfim Santos et al., 2021) including from 100 nuclear loci (Liu et al., 2019). Thus, we restrict a monophyletic Dicranales to a set of core families and accommodate the remaining suite of lineages spanning between the Archidiales and Pottiales in the moss phylogeny (Figure 2; Appendices S4, S7) in new orders. The relationships among these are recovered by a large plurality or a majority of loci, although concordance factors of genes and sites are typically low (Figure 2).

Within liverworts, we propose accommodating the families traditionally included in the Jungermanniales and Porellales (Crandall-Stotler et al., 2009a, b) into five orders each. The Jungermanniales and Porellales s.l. are recovered here as monophyletic (Figure 2; albeit with ambiguity for the latter due to the affinities of the Ptilidiales, see also Dong et al., 2022a, b) and are estimated to have originated in the early Carboniferous. Their subsequent diversification, resulting in their respective five lineages, took place as early as the Late Carboniferous but primarily in the Triassic and

TABLE 1 Synopsis of proposed systematic and nomenclatural changes to the classification of liverworts and mosses (* Newly proposed orders in taxonomic treatment; **resurrected orders [**as in Figure 2]).

Taxonomic group	Reference classification	Proposed accommodation
Liverworts	Crandall-Stotler et al. (2009a, b)	
Cephaloziineae Schljakov	Jungermanniales H. Klinggr.	Lophoziales Schljakov**
Frullaniaceae Lorch in G. Lindau	Porellales Schljakov	Frullaniales D. Bell & D.G. Long*
Jubulaceae H. Klinggr.	Porellales Schljakov	Jubulales Zodda**
Lejeuneaceae Rostovzev	Porellales Schljakov	Lejeuneales Bechteler et al.*
Lophocoleineae Schljakov	Jungermanniales H. Klinggr.	Lepidoziales Schljakov**
Myliaceae Schljakov or Myliineae	Jungermanniales H. Klinggr.	Myliales D.G. Long & D. Bell*
Perssoniellineae R.M. Schuster	Jungermanniales H. Klinggr.	Perssoniellales Schljakov**
Radulineae R.M. Schuster	Porellales Schljakov	Radulales Stotler & Crand.-Stotl.**
Mosses	Goffinet et al. (2009b)	
Amphidiaceae M. Stech	Dicranales H. Philib. ex M. Fleisch.	Amphidiales D. Bell & Goffinet*
Bruchiaceae Schwägr.	Dicranales H. Philib. ex M. Fleisch.	Bruchiales Goffinet*
Distichiaceae Schimp.	Dicranales H. Philib. ex M. Fleisch.	Distichiales D. Bell & Goffinet*
Ditrichaceae Limpr. ^a	Dicranales H. Philib. ex M. Fleisch.	Ditrichales D. Bell & Goffinet*
Erpodiaceae Broth.	Dicranales H. Philib. ex M. Fleisch.	Erpodiales Goffinet*
Eustichiaceae Broth.	Dicranales H. Philib. ex M. Fleisch.	Eustichiales Goffinet*
Flexitrichaceae Ignatov & Fedosov ex D. Bell & Goffinet	“Protohaplolepidae” ^b	Flexitrichales D. Bell & Goffinet*
Leucobryaceae Schimp.	Dicranales H. Philib. ex M. Fleisch.	Archidiales Limpr.
Micromitriaceae Goffinet & Budke	Dicranales H. Philib. ex M. Fleisch.	Archidiales Limpr.
Pleurophasceae Broth.	Pottiales M. Fleisch.	Pleurophascales Goffinet*
Rhabdoweisiaceae Limpr.	Dicranales H. Philib. ex M. Fleisch.	Rhabdoweisiales D. Bell & Goffinet*
Rhachithecaceae H. Rob.	Dicranales H. Philib. ex M. Fleisch.	Rhabdoweisiales D. Bell & Goffinet*
Sorapillaceae M. Fleisch.	Hypnales (M. Fleisch.) W.R. Buck & Vitt	Sorapillales Goffinet*

^aNom. cons. over Ceratodontaceae (Magill, 1977).

^bInformal name first introduced by Hedderson et al. (2004).

Permian, which is more in line with ordinal ages in mosses (Figure 3). A single, universal temporal criterion cannot be applied to individual ranks across the tree of life (see Lücking, 2019), given that the evolution of lineages spans different, although overlapping, periods of time (e.g., ferns and flowering plants). However, mosses and liverworts compose sister lineages that diversified in parallel over the same amount of time (Figure 3), and hence the ranks used in their classification, could be better harmonized along a geological time scale (Appendix S1, Table S9).

Recognizing the main lineages of Jungermanniales or Porellales s.l. (i.e., sensu Crandall-Stotler et al., 2009a, b) at the ordinal rank aligns the crown ages of orders of liverworts more with those of mosses (Figure 3). The lineages segregated from the Porellales s.s. are phenotypically highly similar despite their old divergences, implicitly drawing attention to potential diagnostic innovations other than in morphology, such as ecophysiological and metabolic innovations, as argued for bryophytes in general by Glime (1990).

Phylogenetic relationships within hornworts

The circumscription and relationships among orders within the hornworts, Anthocerotophyta (Figure 2; Appendices S2, S5) are supported by a large majority of loci, in trees built from either nucleotides (Appendix S2) or amino acids (Appendix S5) and are consistent with those inferred previously from analyses of organellar markers and a broad taxon sampling (Villarreal and Renner, 2012). The lone exception is the placement of the monospecific *Leiosporoceros* (node 2; Figure 2). *Leiosporoceros* is sister to all other hornworts in the tree inferred from the ML analysis of the concatenated nucleotide data. This position was previously proposed based on analyses of a few organellar loci sampled for a large set of taxa (Duff et al., 2007; Villarreal et al., 2015; Bell et al., 2020) and from over 400 loci sequenced for selected hornwort placeholders (Leebens-Mack et al., 2019). However, *Leiosporoceros* is sister to the Anthocerotales (i.e., *Anthoceros*) in the ASTRAL tree here based on nucleotide data (Figure 2; Appendix S2), and its placement is ambiguous in the ASTRAL tree inferred from amino acid gene trees (Appendix S5).

Phylogenetic relationships within liverworts

The phylogeny recovers that the earliest split within liverworts separates the Haplomitriopsida (i.e., Calobryales and Treubiales) from the lineage containing the Marchantiopsida (mostly complex thalloid taxa) and the Jungermanniopsida (simple thalloid and leafy liverworts), a topology supported by a small majority of loci (Figure 2; Appendices S3, S6). The Haplomitriopsida (node 10; Figure 2) are morphologically distinct from other liverworts, comprising plants with leaf-like appendages, stems

secreting copious mucilage and one primary androgonial initial in early ontogeny (Crandall-Stotler et al., 2009a). Within the three classes, the ordinal circumscriptions and relationships we report are generally consistent with those of earlier studies (Forrest et al., 2006; Laenen et al., 2014; Villarreal et al., 2016; Yu et al., 2020; Dong et al., 2021, 2022a, b), with many branches supported by a majority of loci, high ML bootstrap values and high local posterior probabilities (Figure 2; Appendices S3, S6).

The earliest split in the Marchantiopsida segregates the Marchantiidae (complex thalloids) from the Blasiidae (node 12; Figure 2), a lineage of two simple thalloid species with endophytic cyanobacteria (Renzaglia and Duckett, 1987; Liaimer et al., 2016). The Marchantiidae (node 13; Figure 2) typically develop a thallus with a distinct epidermis and parenchyma, air chambers, four primary androgonial initials in early ontogeny, and unlobed sporocytes (Crandall-Stotler et al., 2009a). The ordinal relationships within the Marchantiidae vary in support (Figure 2; Appendices S3, S6). The Marchantiales (node 16; Figure 2) contain the majority of its species (ca. 497 spp.), including the model species *Marchantia polymorpha* (Bowman et al., 2017). The Neohodgsoniales mark another deep split in the subclass (Villarreal et al., 2016) and comprise a single species from New Zealand, diagnosed by a uniquely branched carpocephalum (Crandall-Stotler et al., 2009a). The Sphaerocarpaceae (node 15; Figure 2) comprise mostly taxa with leafy-like or winged gametophytes (Crandall-Stotler et al., 2009a) and are sister to the Marchantiales, although this is only supported by a plurality of gene trees (node 14; Figure 2; Appendices S3, S6).

The Jungermanniopsida include species with simple thalloid or leafy gametophytes, and with antheridia developed from two primary androgonial initials in early ontogeny and with lobed sporocytes (Crandall-Stotler et al., 2009a). The Jungermanniopsida (node 17; Figure 2) are typically split into three subclasses (i.e., Pelliidae, Metzgeriidae, and Jungermanniidae; Crandall-Stotler et al., 2009a), whose monophyly and relationships are not consistently resolved (nodes 18, 19, 20, and 22 in Figures 2 and 3). The Metzgeriidae (node 23; Figure 2), composed of the Metzgeriales and Pleuroziales (Figure 2; Appendices S3, S6), are resolved as monophyletic as previously reported from analyses of a few DNA loci (Davis, 2004; He-Nygrén et al., 2004; Forrest et al., 2006), and genomic, transcriptomic, and organellar data (Yu et al., 2020; Dong et al., 2021, 2022a, b). The monophyly of the Metzgeriidae is defined by the uniquely shared lenticular apical cell giving rise to the bilaterally symmetric and thalloid body of the Metzgeriales and the leafy stem of the Pleuroziales (Davis, 2004; He-Nygrén et al., 2004; Forrest et al., 2006; Bell et al., 2020). The subclass Pelliidae traditionally defined based on morphological traits, are by contrast most likely paraphyletic. Within Pelliidae, as traditionally defined, the orders Pallaviciniales (node 21; Figure 2) and Pelliiales (node 28; Figure 2) are monophyletic, while the Fossombroniales are supported by most

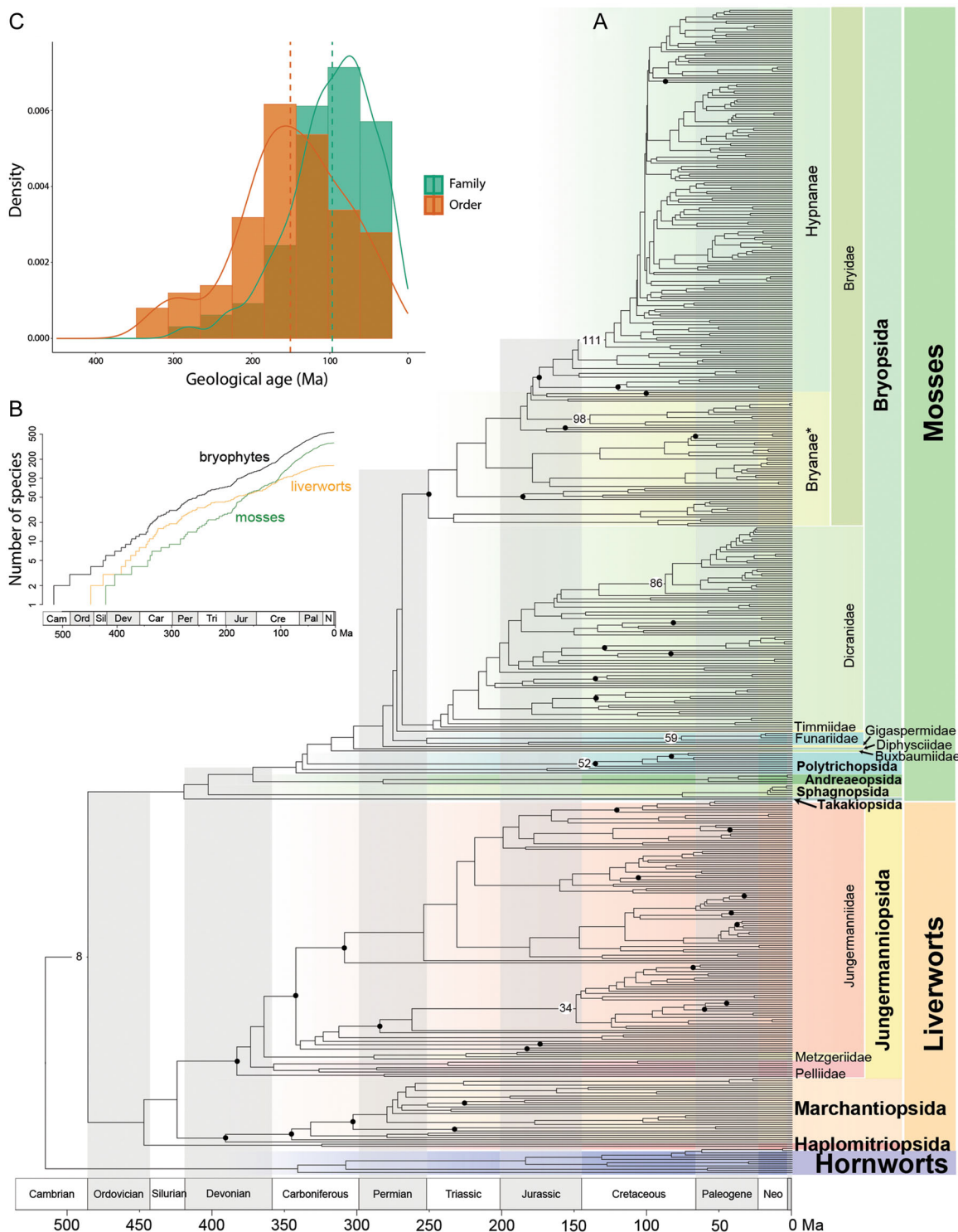


FIGURE 3 (A) Divergence time estimates for bryophytes inferred by penalized likelihood using 29 fossil calibrations. The three bryophyte groups (hornworts, liverworts, mosses) are included with their major suprafamilial taxonomic ranks including classes, subclasses, orders, and suborders. Black dots scattered in the tree represent calibration points (Appendix S1, Table S2). The detailed chronogram with mean node ages including confidence intervals is reported in Appendix S8. Numbers on select nodes match those in Figure 2 and refer to lineages whose diversification in the Cretaceous is discussed in the text. (B) Lineage through time plots of all bryophytes (black line), liverworts (orange line), and mosses (green line), reflecting the slowdown in diversification in liverworts during the Late Cretaceous when compared to mosses. (C) Histogram of the frequency of orders and families estimated from crown age divergences of all bryophytes (hornworts, liverworts, and mosses). Kernel density plots depict the probability distribution (95% confidence interval) of crown age divergences. The green dotted line represents the average of family crown ages and orange dotted line represents the average of order crown ages. See also Appendix S1, Table S9.

nucleotide gene trees but only by a small plurality of amino acid loci (Appendices S3, S6). The Pelliales are sister to all other Jungermanniopsida based on nucleotide data (as in Bell et al., 2020) (Figures 2 and 3; Appendix S3) versus sister to other Pelliidae based on amino acid data with ambiguous signal (Appendix S6). Such conflicting topologies were previously recovered based on nucleotide-based nuclear transcriptome and mitochondrial data (Leebens-Mack et al., 2019; Dong et al., 2021, 2022b), and plastid data (Yu et al., 2020; Dong et al., 2021), respectively.

The vast majority of liverworts (ca. 6160 spp.) belong to the Jungermanniidae, or true leafy liverworts (node 22; Figure 2; Appendices S3, S6). Based on ASTRAL analyses of amino acid data, the Ptilidiales are sister to the Jungermanniales s.l. (Appendix S6, see below for the definition of Jungermanniales s.s.), a placement also supported previously by mitochondrial data (Bell et al., 2020; Dong et al., 2022a; following corrections for edited sites) and plastid-based inferences (Forrest et al., 2006; Yu et al., 2020), but contradicted by our nucleotide analyses and some phylotranscriptomic (Dong et al., 2022b) and plastid studies (Dong et al., 2021), which resolve the Ptilidiales as sister to Porellales s.l. (Figure 2; Appendix S3). A plurality of genes supports the monophyly of the Porellales s.l., which we propose, based on the rationale presented above, to split into five orders (Figure 2; Appendix S3, S6), including the Porellales s.s. (see below for their circumscription), two resurrected orders (Jubulales Zodda and Radulales Stotler & Crand.-Stotl.), and two new orders (Frullaniales and Lejeuneales; see taxonomic treatment below). In our analysis, these orders diverged in the Carboniferous and Permian (Figure 3) and diversified mostly during the late Jurassic and early Cretaceous. The Frullaniales (ca. 599 spp.) and Lejeuneales (ca. 1900 spp., node 34; Figure 2) comprise two of the most species-rich families of liverworts characteristic of epiphytic communities, particularly in tropical rainforests (Feldberg et al., 2014).

The Jungermanniales s.l. comprise five lineages, currently treated at the familial rank, that we propose to recognize at the ordinal level: the previously recognized Perssoniellales, Lepidoziales, and Lophoziales (Schljakov, 1972), Jungermanniales s.str., and a new order, Myliales (see taxonomic treatment below). We resolve the Perssoniellales (ca. 88 spp.) as sister to the remaining orders (node 35; Figure 2). The Myliales (5 spp.) mark the next split based on nucleotide data (Figures 2 and 3; Appendix S3) or are sister to the Lophoziales only, based on amino acid data, although with low support (Appendix S6). *Mylia* was historically considered a member of the Jungermanniaceae (e.g., Crandall-Stotler and Stotler, 2000; Crandall-Stotler et al., 2009a, b) but resolved, based on phylogenetic inference from DNA data, as sister to the remainder of the Jungermanniales s.l. and hence accommodated within the suborder Myliineae (Shaw et al., 2015). The recently proposed sister relationship between *Mylia* and the Jungermanniales s.s. (Dong et al., 2022a) was based on a mislabeled specimen (Y. Liu, Shenzhen Fairy Lake Botanical

Garden, personal communication, March 2023). A majority of nucleotide, and at least a plurality of amino acid, gene trees resolve the Lophoziales (ca. 611 spp., node 38, Figure 2), Lepidoziales (ca. 1943 spp., node 41, Figure 2) and Jungermanniales s.s. (ca. 565 spp., node 40, Figure 2) as monophyletic (Appendices S3, S6, respectively). All three orders are highly heterogeneous in terms of leaf morphology (0–4 lobes), branching patterns, form and position of gametangia (Crandall-Stotler et al., 2009b). The sister-group relationship of the latter two orders, which was also recovered from analyses of nuclear transcriptomic (Dong et al., 2022b) and organellar data (Davis, 2004; Forrest et al., 2006; Dong et al., 2021, 2022a), is supported by a near majority of nucleotide loci but only a weak plurality of amino acid loci (Appendices S3, S6, respectively). The resolution within orders varies, especially within species-rich families (e.g., Lepidoziaceae), potentially as a result of rapid diversification (Appendices S3, S6).

Phylogenetic relationships within mosses

We recovered a phylogenetic tree of the mosses (Figure 2; Appendices S4, S7) that is congruent with most current ordinal relationships based on variation in sporangial dehiscence, peristome architecture and development, and by vegetative body plant organization relative to sex organ position (Liu et al., 2019). We found that the circumscription and relationships of classes and subclasses sensu Goffinet et al. (2009a, b; Liu et al., 2019) were typically supported by a majority or a plurality of loci (Figure 2, Appendix S4) or their amino acid translations (Appendix S7), while concordance among nucleotide loci was typically low for clades following the initial splits within the Bryophyta (Figure 2; Appendix S1, Tables S3, S7).

Our analyses support the current classification (Goffinet et al., 2009a, b) of mosses into five subdivisions (or subphyla identified by their orders in Figure 2). The Takakiophytina (i.e., Takakiales, node 43; Figure 2) are sister to all other extant mosses, followed by the Sphagnophytina (i.e., Sphagnales, node 44; Figure 2), and the lantern mosses (i.e., Andreaeophytina–Andreaeales (node 37; Figure 2) and Andreaebryophytina–Andreaebryales), which are sister to the Bryophytina (all other mosses, node 48; Figure 2), the subdivision containing the majority of moss diversity (Figure 2; Appendices S4, S7). The Bryophytina comprise species potentially developing a peristome, a set of teeth lining the sporangial mouth and controlling spore dispersal (Goffinet et al., 2009b), and stomata on their sporangia. Thus, the lack of stomata in the other four moss subdivisions presumably result from independent losses (Harris et al., 2020), in parallel to losses in the ancestor to liverworts and in two hornwort orders (i.e., Notothyladales and Dendrocerotales; Duff et al., 2007; Villarreal et al., 2015).

Variation in the peristome development and structure mark the major clades within the Bryophytina. Mosses that develop peristome teeth made of whole cells (i.e.,

nematodontous peristome, Figure 1K) form a monophyletic group composed of the Polytrichales (node 52; Figure 2) and Tetrarchidales (node 51; Figure 2) based on a small plurality of nucleotide genes (Figure 2), as previously suggested (Liu et al., 2019). The monospecific Oedipodiales are either sister to all peristomate mosses based on a small plurality of nucleotide gene trees (node 48; Figure 2; Appendix S4) and consistent with previous studies of organellar loci (Chang and Graham, 2014; Liu et al., 2019), or sister to the Polytrichales and Tetrarchidales based on a small plurality of amino acid gene trees (Appendix S7). The ambiguous placement of the Oedipodiales from nucleotide data is likely a combination of a relatively rapid divergence (Figure 3) and saturation in nucleotide substitution because the amino acid data more strongly support the Oedipodiales as sister to the Polytrichales and Tetrarchidales, similar to inferences from amino acid vs. nucleotide data of a distinct set of 105 nuclear loci (Liu et al., 2019).

The remaining mosses (i.e., Bryopsida, node 53; Figure 2) typically develop a peristome composed solely of cell plates rather than whole cells (Figure 1L). The articulated, or arthrodontous, teeth line the sporangial mouth and may respond hygroscopically to regulate dehiscence (Ingold, 1959), so that spores are released when the humidity is optimal for dispersal. Several distinct arthrodontous peristome types arise from cell division patterns established early in sporophyte development (Goffinet et al., 2009b), and these largely define monophyletic groups (Liu et al., 2019). Although evolutionary reductions of the peristome are common across the Bryopsida and may be associated with habitats that favor reduced dispersal (Vitt, 1981), the fundamental developmental sequences underlying fully developed peristomes are likely highly conserved.

The vast majority of mosses belong to the Bryidae, a lineage diagnosed by its double peristome of alternating inner and outer teeth (Goffinet et al., 2009b). This subclass contains the most species-rich superorder of mosses, the Hypnanae (node 103; Figure 2) or pleurocarpous mosses (ca. 4903 spp.) (Crosby et al., 1999), which are characterized by a homogenous midrib anatomy and the lateral development of female sex organs (Bell et al., 2007; Huttunen et al., 2018). Relationships among the five orders of Hypnanae (i.e., Hypnodendrales, Ptychomniales, Hypopterygiales, Hookeriales, and Hypnales) matched those recovered by Liu et al. (2019), but were supported by only a plurality of loci (Figure 2; Appendices S4, S7). While a lateral shift of the sex organs and the associated shift to monopodial growth has occurred in other moss lineages (La Farge-England, 1996), such as the Orthotrichales (node 98; Figure 2), the persistence of lateral female sex organs in all Hypnanae suggested that this trait is either under strong genetic constraint or stabilizing selection (see Coudert et al., 2015, 2017).

Within the Hypnales (node 111; Figure 2), the backbone relationships are typically shared only by a plurality of gene trees (Figure 2; Appendices S4, S7), likely reflecting a rapid

early radiation (Shaw et al., 2003). We found that several species-rich, morphologically defined families are either paraphyletic, due to the inclusion of additional, morphologically distinct lineages, or polyphyletic with taxonomically defining features evolving in multiple distantly related lineages. The lack of concordance between the morphology-based systematic concepts and the phylogeny based on our phylogenomic data indicates that gametophyte morphology is evolutionarily highly labile within the Hypnales. Gametophytic traits that are taxonomically useful in other lineages of mosses are highly homoplasious in this group, due to shifts in habitats following speciation (Huttunen and Ignatov, 2010), or hybridization (Sawangproh et al., 2020), or even highly variable along ecological gradients (Spitale and Petraglia, 2010), or potentially due to incomplete lineage sorting. Remarkably, the homoplasy we observed may even span across subclasses. *Sorapilla*, the sole member of Sorapillaceae, was originally placed in the Dicranidae, but was then moved to the Hypnales, where it currently resides with unknown affinities (Meagher et al., 2020). Based on the first DNA sequences obtained for this genus, we resolve the Sorapillaceae in the Dicranidae as proposed earlier (Lin, 1983; Vitt, 1984) but in an isolated position within the Dicranalean grade (Figure 2; Appendices S4, S7), prompting us to propose a new order, Sorapillales, for it (see taxonomic treatment below).

The pleurocarpous Hypnanae evolved from an acrocarpous ancestor in the Bryidae, typically characterized by at least female sex organs terminating the stem. The acrocarpous Bryidae are historically placed within the Bryanae, a group that we and prior molecular analyses (e.g., Cox et al., 2010; Liu et al., 2019) recovered as paraphyletic (Figure 2; Appendices S4, S7). While we found strong support for the monophyly of all recognized orders in the Bryanae, the relationships among them were typically supported only by a plurality of loci (Figure 2; Appendices S4, S7). The relationships among the Rhizogoniales (node 96; Figure 2), Orthotrichales, Orthodontiales (node 100; Figure 2), and Aulacomniales (node 102; Figure 2) inferred from nucleotide data (Figure 2; Appendix S4) match those previously proposed (Liu et al., 2019). However, the amino acid data (Appendix S7) support a clade comprising some members of the Rhizogoniales, along with *Hymenodontopsis*, a member of the Aulacomniaceae, as sister to the Hypnanae, whereas the Orthotrichales, Orthodontiales, Aulacomniales, and *Goniobryum* (a member of the Rhizogoniaceae) compose a single lineage sister to the Rhizogoniales and Hypnanae (Appendix S7). The relationships of these orders are in all cases supported only by a small plurality of loci.

The genus *Calomnion* (node 105; Figure 2), a member of the Rhizogoniales (Bell et al., 2007) and consisting of a few South Pacific Island species (Vitt, 1995), was either sister to the Hypnanae, minus the Hypnodendrales, or all Hypnanae based on nucleotide or amino acid data, respectively (Figure 2; Appendices S4, S7). None of the alternative topologies are supported by a majority of loci, and hence the

circumscription of the Rhizogoniales remains uncertain. Similarly, the early diversification of the Bryidae gave rise to the Bartramiales (node 92; Figure 2), Bryales (node 94; Figure 2), Hedwigiales (node 89; Figure 2), and Splachnales (node 91; Figure 2), which individually are strongly supported as monophyletic, but the relationships among these orders are still uncertain here. The Helicophyllaceae (Hedwigiales), diagnosed by plagiotropic shoots and dimorphic leaves (Vitt, 1982), are resolved as sister to the Bartramiaceae (Figures 2 and 3; Appendices S4, S7) as previously suggested by Buchbender et al. (2014).

The Dicranidae, which are defined by their peristome composed of a single ring of peristome teeth homologous to the inner ring of the Bryidae peristome, are strongly supported as sister to the Bryidae (Figure 2). The ordinal phylogeny in our analyses is consistent with previous studies (Cox et al., 2010; Liu et al., 2019) in showing that the morphologically defined Dicranales are highly polyphyletic. The earliest splits within the subclass gave rise to the Catoscopiales, followed by the newly erected Distichiales and Flexitrichales (see taxonomic treatment below). The latter holds only the Flexitrichaceae (a family here formally recognized; see taxonomic treatment below) and is likely sister to an unsampled Scouleriales sensu Fedosov et al. (2016) (Figure 2). The next split yields the Grimmiales, sister to the clade composed of the Archidiales, the paraphyletic Dicranales s.l., and the Pottiales (Figure 2; Appendices S4, S7). Here we broaden the circumscription of the Archidiales to include the Micromitriaceae and Leucobryaceae because the Archidiaceae are nested between the latter two families (Figure 2; Appendices S4, S7) as previously suggested based on organellar loci (Bonfim Santos et al., 2021).

The Dicranales s.l. are consistently resolved as paraphyletic to a well-supported Pottiales (node 84; Figure 2; Appendices S4, S7), which is congruent with previous phylogenetic studies (Liu et al., 2019; Bonfim Santos et al., 2021; Fedosov et al., 2021). Based on the well-supported relationships here, we propose to restrict the Dicranales (Figure 2) to only the Dicranaceae, Calymperaceae, Fissidentaceae, and Octoblepharaceae and accommodate the remaining families (Appendix S4) on topological grounds in the Amphidiales, Bruchiales, Ditrichales, Erpodiales, Eustichiales, and Rhabdoweisiales (see taxonomic treatment below). Our sampling, however, is insufficient to resolve the placement of all families in the Dicranales s.l., and so families such as the Aongstroemiaceae and Dicranellaceae (Bonfim Santos et al., 2021; Fedosov et al., 2023) remain unassigned. The Pleurophascaceae, a monogeneric family endemic to Australasia (Fife and Dalton, 2005), is the sole member of the Pottiales sensu Goffinet et al. (2009b) to be consistently resolved outside of the order (Figure 2), although with ambiguous affinities given the incongruence in topologies inferred from nucleotide versus amino acid data (Appendix S4 vs. S7, respectively). All analyses resolve the family within the Dicranidae (Figure 2), in contrast to Goffinet et al. (2001) who

proposed, based on a single and partial plastid sequence, that *Pleurophascum* belonged to the Bryidae, a resolution that was considered likely artefactual by Stech et al. (2012).

Our phylogenomic inferences confirm that the Timmiidae (node 60; Figure 2), restricted to *Timmia* and characterized by a unique peristomial architecture of 64 endostomial filaments (Budke et al., 2007), compose the sister lineage to the ancestor of the Dicranidae and Bryidae (Liu et al., 2019). The Funariidae (node 59; Figure 2), which include the model taxon *Physcomitrium patens* (Medina et al., 2019; Rensing et al., 2020) along with the Diphysciidae and Buxbaumiidae, each with a distinct peristome type (Shaw et al., 1987; Ignatov et al., 2018) are successively sister to other lineages in the Bryopsida (nodes 53–56, 60; Figure 2). Thus, the main transformations of the arthro-dontous peristome, yielding the various fundamental types, occurred during the Permian or even early Triassic (Figure 3; Laenen et al., 2014). Although diagnostic of subclasses of the Bryopsida (Goffinet et al., 2009b) these distinct peristome architectures can be variously modified and reduced, especially along environmental gradients (Vitt, 1981).

Gene tree discordance

The multilocus nuclear data set from the GoFlag 408 flagellate land plant probes also enables deeper insights into the processes generating genetic conflict among loci than was possible in previous phylogenetic analyses of moss diversity based mostly on organellar sequence data. Across the phylogeny, we identified numerous nodes with extensive gene tree discordance (Figure 2; Appendices S1 [Tables S3–S7], S9, S10). Such discordance may arise due to either systematic error in the analyses, such as model misspecification, or stochastic error in tree reconstruction (Degnan and Rosenberg, 2009), which likely plays a role in our analyses because the target exons in the GoFlag probe set are relatively conserved and many of the locus alignments are short. Alternately, biological sources like horizontal gene transfer, unrecognized paralogy, incomplete lineage sorting (ILS; Degnan and Rosenberg, 2009; Morales-Briones et al., 2021), or hybridization (Stull et al., 2023) could contribute to the incongruence. In the bryophytes, ILS may be associated with rapid radiations, and there is also evidence of reticulation events within and between classes of liverworts (Dong et al., 2022a). Although these biological processes may leave a characteristic signature, in practice it is often difficult to definitively identify the factor (s) driving gene-tree species-tree conflict or distinguish them from analytical error, especially at such a large scale.

In the ASTRAL nucleotide tree, 173 nodes (of 531 nodes total) have high gCF values (>50%), and 192 have high sCF values (>50%), strongly supporting these nodes in the species tree (Figure 2; Appendix S1, Tables S4, S7). In contrast, 254 nodes have low gCF values (<33%), and these appear especially common among the backbone nodes

(Appendix S1, Table S4). Most (224) of the 254 nodes with low gCF values had gDFP values over 50% (up to 99.56%), which indicate high rates of paraphyly or lack of information in the loci. High gDFP values suggest potentially high rates of error in the gene tree inference may be contributing to much of this discordance. For 217 of those 254 nodes, gDF1 and gDF2 were not significantly different ($\chi^2 > 0.05$), and sDF1 and sDF2 were not significantly different in 135 of these nodes. The results are consistent with high levels of ILS, but error is also likely contributing to much of this discordance.

When we focus on 111 nodes across the backbone and immediately subsequent nodes (numbered in Figure 2; Appendix S1, Table S4), 50 of these nodes have low gCF (<33%), and 27 have low sCF values (<33%), indicating high levels of discordance, especially in the backbone (Figure 2). In many of these cases, the gDFP values (yellow in pie charts, Figure 2) are elevated, again indicating a lack of a clear phylogenetic signal in the corresponding parts of the gene trees. In hornworts, a single node (node 2, the split between *Leiosporoceros* and Anthocerotales) shows low gCF and sCF as well as nearly equal quartets in the ASTRAL tree, consistent with ILS. In the liverworts, 12 nodes have low gCF values (see Appendix S1, Table S7), including node 19 (split between “Pelliidae” and the remaining liverworts), node 22 (the split between Pleuroziales and Metzgeriales from the rest of the leafy liverworts), node 26 (split between Ptilidiales and the combined Porellales, Radulales, Frullaniales, Jubulales, and Lejeuneales), node 28 (split between Porellales and the combined Radulales, Frullaniales, Jubulales, and Lejeuneales), node 30 (split between Radulales and the combined Frullaniales, Jubulales, and Lejeuneales) and node 39 (split between Jungermanniales and Lepidoziales). In mosses, 37 nodes have low gCF values (see Appendix S1, Table S7), including node 49 (split between Tetrarchidiales and Polytrichales and the rest of the mosses), node 61 (split between Dicranidiidae and their sister lineage); node 63 (split between Distichiales and the other mosses), node 84 (the split between Ditrichales and Pottiales), node 88 (split between Splachnales from the remaining Bryidae), and node 103 (split of the Hypnodendrales from remaining Hypnanae). In the majority of the 37 moss nodes with low GCF values, we cannot reject the null hypothesis of equal frequencies of the alternate topologies ($\chi^2 > 0.05$), suggesting little evidence of reticulation among these lineages.

Although this study does not explore the causes of gene tree discordance in depth, the high levels of discordance throughout the tree highlight both the likely complexity of bryophyte diversification and the difficulty of resolving bryophyte relationships. It also emphasizes the dangers of relying on phylogenetic trees inferred from one or few loci. The multigene data set provides not only more power to resolve difficult relationships, but more importantly enables us to account for what appears to be high levels of historical variation throughout the genome in our evolutionary inferences.

Divergence times and rates of molecular evolution

The divergence time estimates support that the bryophytes arose in the late Cambrian-Ordovician, in line with Morris et al. (2018; but see Bowman, 2022; McCourt et al., 2023). The most species-rich lineages of extant bryophytes (e.g., Hypnales [node 111; Figure 3], Lejeuneales [node 34; Figure 3]) diversified in parallel with the angiosperms during the Cretaceous (Figure 3; Appendices S8, S11, S12). The common ancestor to extant lineages of mosses and liverworts is traced to 420 [416–424] Ma and 447 [444–450] Ma, respectively, which is also consistent with recent estimates (Bell et al., 2007; Villarreal and Renner, 2012; Feldberg et al., 2014; Morris et al., 2018; Harris et al., 2022). The lineage through time plots (Figure 3B) suggest a steady diversification of both lineages over the last 400 Ma with a higher net moss diversification in the mid-Cretaceous.

The average crown age of orders as recognized here across all three bryophyte lineages is 150.5 Ma (SD 70 Ma) (Figure 3C; Appendix S1, Table S9). The crown age of the Hypnales (491 genera, ca. 4150 species; node 111 in Figure 3) is 129 [78–173] Ma, younger than was previously estimated (Newton et al., 2007). We reconstructed the origin of mosses and liverworts (419–447 Ma, crown group Setophyta; node 8 in Figure 3) as slightly older than that of extant lycophytes and their sister group, the euphyllophytes (Morris et al., 2018). The age of most bryophyte orders coincides with the diversification of angiosperms during the Late Jurassic and Cretaceous (Lloyd et al., 2008).

Our estimates of family stem ages suggest that most bryophyte families (63% of families, $N = 166$) originated during the Cretaceous (65 families) or Jurassic (40 families). Extant bryophyte families (crown ages, $N = 80$) diversified predominantly during the Early Cretaceous (103–145 Ma, 18 families), the Late Cretaceous (66–102 Ma, 27 families), or the Cenozoic (–65 Ma, 26 families). The average crown age of bryophyte families was 98 Ma (SD 51 Ma) (Appendix S1, Table S9; Appendices S8, S11, S12). In mosses, the crown age of the Pottiaceae (77 genera, ca. 1209 species; node 86 in Figure 3) was estimated at 133.3 (115–150) Ma, while the Orthotrichaceae (24 genera, ca. 900 species; node 98 in Figure 3) started to diversify around 139.6 (106–169) Ma. Within liverworts, the diversification of the hyperdiverse Lejeuneaceae (ca. 88 genera, ca. 1900 species; node 34 in Figure 3) began around 149 (116–188) Ma, while the origin of the Lepidoziaceae (31 genera, ca. 703 species, Appendix S8) dates to 121 (114–166) Ma. As previously suggested for bryophyte genera (Laenen et al., 2014), bryophyte diversity may have accrued steadily during the Cretaceous and Cenozoic (Figure 3C). Our analyses indicate that the majority of bryophyte families diversified during the Cretaceous terrestrial revolution (Lloyd et al., 2008; Benton et al., 2022; Figure 3; Appendices S1 [Table S9], S8, S11, S12) in parallel with the angiosperms and leptosporangiate ferns (Lovis, 1977; Schuettpelz and Pryer, 2009). Indeed, the climatic fluctuations during the Cretaceous and Cenozoic may have

triggered the burst of diversity in lineages in arid regions (e.g., Pottiales, node 86; Figure 3) or exposed habitats (e.g., Funariales, node 59, Figure 3; Polytrichales, node 52, Figure 3) before the subsequent explosive diversification of angiosperms and ferns (Schuettpelz and Pryer, 2009).

The phylogenomic chronogram of the bryophytes enables us to estimate the absolute rates of nuclear loci for 46 major clades based on the nuclear exons generated from the GoFlag flagellate land plant probe set (Appendix S1, Table S10). Our chronogram provides a framework to infer the timing of speciation events for fossil-poor families such as the Funariaceae (including *Physcomitrium*) or ecologically important genera such as *Hylocomium*, *Pleurozium*, and *Sphagnum*. Lineage rate variation is expected across such a broad phylogenetic spectrum. The lowest absolute substitution rate in mosses characterizes the Orthodontiales (1.34E-04 substitutions per site per Ma [subst/site/Ma]) and the highest the Polytrichales (5.44E-04 subst/site/Ma). In liverworts, the variation spans from 3.53E-04 subst/site/Ma in the simple thalloid Pallaviciniales to 7.85E-04 subst/site/Ma in the complex thalloids (Marchantiopsida) (Appendix S1, Table S10). The latter is striking given that the organellar absolute substitution rate in complex thalloids is the slowest among all extant liverworts (2.63 E-04 subst/site/Ma; Villarreal et al., 2016). The nuclear rates recovered in our analyses span the known absolute rates found in seed plants (De La Torre et al., 2017). The rate variation observed in our data set sets the stage to test specific hypotheses correlating life history traits (e.g., perennial vs annual taxa, monoicous vs dioicous sexual systems) and molecular rates across bryophyte groups and also is inconsistent with traditional ideas that bryophytes, as a whole, represent a slow-evolving lineage compared to vascular plants (Crum, 1972, 2001).

TAXONOMIC TREATMENT

Marchantiophyta (Liverworts)

Lejeuneales Bechteler, A.M. Sierra, & D.G. Long ord. nov.

Leaves mostly 2-lobed, the ventral lobule usually attached to the dorsal lobe along the ventral margin forming a keel perpendicular or oblique to the stem, forming an inflated but not galeate water sac with its longer axis usually roughly parallel to the ventral margin of the dorsal lobe, stylus reduced to a slime papilla, gynoecia with 1 archegonium and a single series of bracts and bracteoles, seta 4 cells in diameter, commonly articulate, capsules spherical with the wall 2-stratose, elaters few, permanently attached to capsule valves. Type: Lejeuneaceae Rostovzev, Morf. Sist. Pechen. Mhov: 94. 1913; Lejeuneaceae.

Frullaniales D. Bell & D.G. Long ord. nov.

Leaves 3-lobed, the median lobule almost free from dorsal lobe, lobule keel parallel to the stem, forming an inflated cylindrical or galeate (rarely explanate) water sac with its longer axis approximately parallel to stem, stylus

present, underleaves bifid (rarely entire), gynoecia with multiple archegonia, bracts and bracteoles in 3 or 4 series, seta up to 12 cells in diameter, non-articulate, capsules spherical with the wall 2-stratose, elaters few, permanently attached to capsule valves. Type: Frullaniaceae Lorch in G.Lindau, Krypt.-Fl. Anf. 6: 174. 1914; Frullaniaceae.

Myliales D.G. Long & D. Bell ord. nov.

Branching mostly terminal, rhizoids numerous, leaves succubous, simple, smooth or ornamented, gemmiferous with 1- or 2-celled gemmae on leaf tips, underleaves reduced, plants dioicous, sporophyte enclosed in shoot calyptra and perianth, perianths laterally compressed above, capsules ovoid with the wall 3- to 5-stratose. Type: Myliaceae Schljakov, Novosti Sist. Nizsh. Rast. 12: 308. 1975; Myliaceae.

Bryophyta (Mosses)

Amphidiales D. Bell & Goffinet ord. nov.

Plants acrocarpous, forming dense cushions, leaves crisped when dry, capsules gymnostomous, emergent to shortly exerted. Type: Amphidiaceae M. Stech, Nova Hedwigia 86: 14, 2008; Amphidiaceae.

Bruchiales Goffinet ord. nov.

Plants erect, acrocarpous, capsule with well-developed neck, peristome haplolepidous (see Buck, 1979). Type: Bruchiaceae Schimp., Coroll. Bryol. Eur.: 6, 1856; Bruchiaceae.

Distichiales D. Bell & Goffinet ord. nov.

Plants acrocarpous, leaves distichous, spreading from broad sheathing base, costa excurrent, monoicous, peristome haplolepidous. Type: Distichiaceae Schimp., Syn. Musc. Eur. 135. 1860; Distichiaceae.

Ditrichales D. Bell & Goffinet ord. nov.

Plants erect, acrocarpous, with costate and mostly lanceolate leaves, sporangium exerted with haplolepidous peristome, or immersed and cleistocarpous. Type: Ditrichaceae Limpr., Laubm. Deutschl. 1: 482, 1887; Ditrichaceae.

Erpodiales Goffinet ord. nov.

Plants small, plagiotropic, leaves ecostate, cladocarpous, peristome haplolepidous (see Pursell, 2017). Type: Erpodiaceae Broth., Nat. Pflanzenfam. I(3): 706. 1905; Erpodiaceae.

Eustichiales Goffinet ord. nov.

Plants erect, leaves single costate, distichous with sheathing laminae, with lateral sporophytes and erect capsules. Type: Eustichiaceae Broth., Nat. Pflanzenfam. (ed. 2) 10: 420, 1924; Eustichiaceae.

Flexitrichaceae Ignatov & Fedosov ex D. Bell & Goffinet fam. nov. for Flexitrichaceae Ignatov & Fedosov invalid

Plants acrocarpous; leaves straight to flexuose, from sheathing bases, dioicous, peristome haplolepidous (see Fedosov et al., 2016). Type: *Flexitrichum* Ignatov & Fedosov, Bot. J. Linn. Soc. 181(2): 152. 2016; *Flexitrichum*.

Flexitrichales D. Bell & Goffinet ord. nov.

Plants acrocarpous; leaves straight to flexuose, from sheathing bases, dioicous. Type: Flexitrichaceae Ignatov & Fedosov ex D. Bell & Goffinet; Flexitrichaceae.

Pleurophascales Goffinet ord. nov.

Plants robust, stems plagiotropic, branches erect, leaves lacking costa, sporophyte exerted, capsule globose, cleistocarpous. Type: Pleurophascaceae Broth. Nat. Pflanzenfam. I (3): 774, 1906; Pleurophascaceae.

Rhabdoweisiales D. Bell & Goffinet ord. nov.

Plants small, erect, acrocarpous, leaves unicostate, lamina unistratose except perhaps at margin, mostly autoicous, peristome haplolepidous (see Fedosov et al. [2021] and Goffinet [1997]). Type: Rhabdoweisiaceae Limpr. Laubm. Deutschl. 1: 271, 1886; Rhabdoweisiaceae (Fedosov et al., 2021) and Rhachitheciaceae H. Rob. (Goffinet, 1997).

Sorapillales Goffinet ord. nov.

Plants monopodial, vaginant leaves distichous, complanate, sporophyte lateral, immersed, peristome haplolepidous with vestigial exostome (see Meagher et al., 2020). Type: Sorapillaceae M. Fleisch, Musci Buitenzorg 3: 847, 1908; Sorapillaceae.

CONCLUSIONS

The phylogenetic relationships that we report based on data generated using the GoFlag 408 flagellate land plant probe set are largely congruent with previous efforts, with some interesting exceptions (Figure 2). The general consistency among studies based on different data and analytical methods suggests that the bryophyte phylogenetic studies are converging on a relatively stable set of relationships. Most of the new orders we circumscribe were evident in earlier studies that lacked either the taxonomic sampling or genetic data to draw firm taxonomic conclusions. The presence of biological conflict among loci also highlights that a single true species tree may be illusory and instead suggests that we reevaluate the questions we wish to answer. If we are interested in species diagnosis, for example, resolving the exact bifurcating relationships among our taxonomic units may not be essential. Alternatively, if we are interested in reconstructing the history of specific ecologically important traits, perhaps the critical information is contained not in the species tree but rather in the history of the genes that govern variation in such traits (Wu et al., 2018). Embracing this topological conflict opens new research avenues to elucidate the processes of diversification in bryophytes.

The phylogenomic data generated from this project, along with the inferred chronogram and rates of evolution, provide a foundational resource for future evolutionary research across the bryophytes and highlights the utility of GoFlag 408 across lineages diversifying for 500 Ma, including for order-level classification. The current challenge facing the community is to fill in the phylogeny with unsampled genera, species, or populations of focal taxa. Expanding the analyses to include the highly variable flanking intron and spacer regions from the GoFlag 408 probe set could provide the resolution for relationships among populations of single species or groups of closely

related species. Indeed, the rapidly growing GoFlag 408 database of sequences provides a sturdy scaffold in which to place more focused studies (Budke et al., 2022; Draper et al., 2022; Jauregui-Lazo et al., 2023). Thus, this study provides a robust framework to further resolve the relationships among bryophytes, reconstruct the evolution of biologically important characters, identify innovations and targets of selection, and elucidate the mechanisms that shape the diversification of bryophytes.

AUTHOR CONTRIBUTIONS

The concept of the study was developed by J.G.B., S.F.M., D.B., G.P.-B., J.B., B.G., and J.C.V.A. B.G., and J.C.V.A. wrote the first draft of the manuscript, which was then reviewed by J.G.B., S.F.M., K.S.R., D.Q., J.L., F.L., I.D., E.B.S., J.B., D.B., G.P.-B., B.G., and J.C.V.A. Specimens were collected by A.B., A.M.S.P., A.S.-V., C.E.Z., E.C.D., D.C.C., I.D., J.J.L., J.L., L.R.L., M.v.K., S.C., S.H., D.L., L.E., L.L.F., P.L., R.G., G.E.L., K.F., J.B., G.P.-B., S.F.M., D.B., J.B., and J.C.V.A. DNA was extracted and data were generated by L.R.L., L.E., G.E.L., J.B., and J.C.V.A., and analyses were performed by J.G.B., J.B., G.P.-B., A.M.S.P., and J.C.V.A. Funding for the study was obtained by J.G.B., E.C.D., E.B.S., S.F.M., and J.C.V.A.

AFFILIATIONS

¹Nees-Institute for Plant Biodiversity, University of Bonn, Meckenheimer Allee 170, 53115 Bonn, Germany

²Plant Biodiversity and Ecology, iES Landau, Institute for Environmental Sciences, RPTU University of Kaiserslautern-Landau, Fortstraße 7, 76829 Landau, Germany

³Laboratório de Sistemática Vegetal, Departamento de Botânica, Instituto de Ciências Biológicas, Universidade Federal de Minas Gerais, Brazil

⁴Royal Botanic Garden Edinburgh, 20A Inverleith Row, Edinburgh EH3 5LR, UK

⁵Department of Biological Sciences, University of Florida, 220 Bartram Hall, Gainesville, FL 32611, USA

⁶California State Polytechnic University, Humboldt, Arcata, CA 95521, USA

⁷Australian National Herbarium, Centre for Australian National Biodiversity Research, GPO Box 1700, Canberra, ACT 2601, Australia

⁸PSU Herbarium, Division of Biological Science, Faculty of Science Prince of Songkla University, Hat Yai, Songkhla 90110, Thailand

⁹Departamento de Biología, Facultad de Ciencias, Universidad Autónoma de Madrid, 28049 Madrid, Spain/Centro de Investigación en Biodiversidad y Cambio Global, Universidad Autónoma de Madrid, 28049 Madrid, Spain

¹⁰Departamento de Botánica y Geología, Universidad de Valencia, Avda. Vicente Andrés Estelles s/n, 46100 Burjassot, Spain

¹¹Department of Botany, University of British Columbia, 6270 University Boulevard, Vancouver, British Columbia V6T 1Z4, Canada

¹²Herbarium (TUR), Biodiversity Unit, 20014 University of Turku, Finland

¹³Department of Plant Biology and Genome Center, University of California Davis, 451 Health Sciences Drive, Davis, CA 95616, USA

¹⁴Centro de Investigación en Recursos Naturales y Sustentabilidad (CIRENYS), Universidad Bernardo O'Higgins, Avenida Viel 1497, Santiago, Chile

¹⁵Department of Plant Biology, Southern Illinois University, Carbondale, IL 62901, USA

¹⁶Mittlere Letten 11, 88634 Herdswangen-Schönach, Germany

¹⁷Faculty of Science and Marine Environment/Institute of Tropical Biodiversity and Sustainable Development, Universiti Malaysia Terengganu, 21020 Kuala Nerus, Terengganu, Malaysia

¹⁸Département de Biologie, Université Laval, Québec, Québec G1V 0A6, Canada

¹⁹Gantz Family Collections Center, Field Museum, 1400 S. DuSable Lake Shore Drive, Chicago, IL 60605, USA

²⁰Instituto Nacional de Pesquisas da Amazônia, Departamento de Biodiversidade, Avenida André Araújo, 2936, Aleixo, CEP 69060-001, Manaus, AM, Brazil

²¹Universidade do Estado do Amazonas, Av. Djalma Batista, 2470, Chapada, Manaus, 69050-010 Amazonas, Brazil

²²Ecology and Evolutionary Biology, University of Connecticut, 75 North Eagleville Road, Storrs, CT 06269-3043, USA

ACKNOWLEDGMENTS

The authors thank all the herbaria that provided specimens. Funding was provided by the NSF collaborative project “Building a Comprehensive Evolutionary History of Flagellate Plants” (DEB #1541506 to J.G. Burleigh, E.C. Davis, S.F. McDaniel, and E.B. Sessa, and #1541545 to M von Konrat). B.G. acknowledges DEB-1753811. J.C.V.A. acknowledges the Canada Research Chair (950-232698); the CRNSG-RGPIN 05967–2016 and the Canadian Foundation for Innovation (projects 36781, 39135). The authors thank the two anonymous reviewers and the Associate Editor for their constructive comments on previous versions of the manuscript.

OPEN RESEARCH BADGES



This article has been awarded Open Data and Open Materials badges. All materials and data are publicly accessible via the Open Science Framework at <https://datadryad.org/stash/dataset/doi:10.5061/dryad.3j9kd51qm>. Learn more about the Open Practices badges from the Center for Open Science: <https://osf.io/tvxyz/wiki>.

DATA AVAILABILITY STATEMENT

The raw sequence reads for all samples have been deposited in the NCBI SRA database (and all SRA accession numbers can be found in Appendix S1, Table S1). All phylogenetic nucleotide and amino acid alignments and resulting gene trees and species trees are available at Dryad: <https://doi.org/10.5061/dryad.3j9kd51qm> (Bechteler et al., 2023).

ORCID

Julia Bechteler <http://orcid.org/0000-0002-5115-657X>

Gabriel Peñaloza-Bojacá <http://orcid.org/0000-0001-7085-9521>

David Bell <http://orcid.org/0000-0002-1059-8777>

J. Gordon Burleigh <http://orcid.org/0000-0001-8120-5136>

Stuart F. McDaniel <http://orcid.org/0000-0002-5435-7377>

Emily B. Sessa <http://orcid.org/0000-0002-6496-5536>

Alexander Bippus <http://orcid.org/0000-0001-8668-0665>

D. Christine Cargill <http://orcid.org/0000-0001-8390-3245>

Sahut Chantanoarrapint <http://orcid.org/0000-0002-9739-0994>

Isabel Draper <http://orcid.org/0000-0003-3102-9386>

Lorena Endara <http://orcid.org/0000-0003-2834-7412>

Laura L. Forrest <http://orcid.org/0000-0002-0235-9506>

Ricardo Garilleti <http://orcid.org/0000-0002-5977-2908>

Sean W. Graham <http://orcid.org/0000-0001-8209-5231>

Sanna Huttunen <http://orcid.org/0000-0003-1374-9857>

Javier Jauregui Lazo <http://orcid.org/0000-0002-6334-325X>

Francisco Lara <http://orcid.org/0000-0002-1665-5277>

Juan Larraín <http://orcid.org/0000-0002-9423-6561>

Lily R. Lewis <http://orcid.org/0000-0001-6529-9785>

David G. Long <http://orcid.org/0000-0003-0816-0124>

Dietmar Quandt <http://orcid.org/0000-0003-4304-6028>

Karen Renzaglia <http://orcid.org/0000-0002-1406-2646>

Alfons Schäfer-Verwimp <http://orcid.org/0000-0002-2720-6055>

Gaik Ee Lee <http://orcid.org/0000-0001-5161-6196>

Adriel M. Sierra <http://orcid.org/0000-0001-9900-1350>

Matt von Konrat <http://orcid.org/0000-0001-9579-5325>

Charles E. Zartman <http://orcid.org/0000-0001-8481-9782>

Marta Regina Pereira <http://orcid.org/0000-0001-7236-2383>

Bernard Goffinet <http://orcid.org/0000-0002-2754-3895>

Juan Carlos Villarreal A. <http://orcid.org/0000-0002-0770-1446>

REFERENCES

- Bechteler, J., G. Peñaloza-Bojacá, D. Bell, J. G. Burleigh, S. F. McDaniel, C. Davis, E. B. Sessa, et al. (2023). Comprehensive phylogenomic time tree of bryophytes reveals deep relationships and uncovers gene incongruences in the last 500 million years of diversification [Dataset]. Dryad. <https://doi.org/10.5061/dryad.3j9kd51qm>
- Bell, D., Q. Lin, W. K. Gerelle, S. Joya, Y. Chang, Z. N. Taylor, C. J. Rothfels, et al. 2020. Organellomic data sets confirm a cryptic consensus on (unrooted) land-plant relationships and provide new insights into bryophyte molecular evolution. *American Journal of Botany* 107: 91–115.
- Bell, N. E., D. Quandt, T. J. O'Brien, and A. E. Newton. 2007. Taxonomy and phylogeny in the earliest diverging pleurocarps: square holes and bifurcating pegs. *Bryologist* 110: 533–560.
- Bennett, T., M. Liu, T. Aoyama, N. Bierfreund, M. Braun, Y. Coudert, R. Dennis, et al. 2014. Plasma membrane-targeted pin proteins drive shoot development in a moss. *Current Biology* 24: 2776–2785.
- Benton, M. J., P. Wilf, and H. Sauquet. 2022. The Angiosperm Terrestrial Revolution and the origins of modern biodiversity. *New Phytologist* 233: 2017–2035.
- Bippus, A. C., J. R. Flores, J. Hyvönen, and A. M. F. Tomescu. 2022. The role of paleontological data in bryophyte systematics. *Journal of Experimental Botany* 73: 4273–4290.
- Bonfim Santos, M., V. Fedosov, T. Hartman, A. Fedorova, H. Siebel, and M. Stech. 2021. Phylogenetic inferences reveal deep polyphyly of Aongstroemiaceae and Dicranellaceae within the haplolepideous mosses (Dicranidae, Bryophyta). *Taxon* 70: 246–262.
- Bouckaert, R., J. Heled, D. Kühnert, T. Vaughan, C.-H. Wu, D. Xie, M. A. Suchard, et al. 2014. Beast 2: a software platform for Bayesian evolutionary analysis. *PLoS Computational Biology* 10: e1003537.
- Bowman, J. L. 2022. The origin of a land flora. *Nature Plants* 8: 1352–1369.
- Bowman, J. L., T. Kohchi, K. T. Yamato, J. Jenkins, S. Shu, K. Ishizaki, S. Yamaoka, et al. 2017. Insights into land plant evolution garnered from the Marchantia polymorpha genome. *Cell* 171: 287–304.
- Breinholt, J. W., S. B. Carey, G. P. Tiley, E. C. Davis, L. Endara, S. F. McDaniel, L. G. Neves, et al. 2021. A target enrichment probe set

- for resolving the flagellate land plant tree of life. *Applications in Plant Sciences* 9: 1–28.
- Brinda, J. C., and J. J. Atwood. 2023. Bryophyte nomenclator [online]. Website: <https://www.bryonames.org> [accessed November 2022].
- Brown, J. W., J. F. Walker, and S. A. Smith. 2017. Phyx: phylogenetic tools for unix. *Bioinformatics* 33: 1886–1888.
- Buchbender, V., H. Hespánhol, M. Krug, C. Sérgio, A. Séneca, K. Maul, L. Hedenäs, and D. Quandt. 2014. Phylogenetic reconstructions of the Hedwigiaceae reveal cryptic speciation and hybridisation in *Hedwigia*. *Bryophyte Diversity and Evolution* 36: 1–21.
- Buck, W. R. 1979. A re-evaluation of the Bruchiaceae with the description of a new genus. *Brittonia* 31: 469–473.
- Budke, J., C. Jones, and B. Goffinet. 2007. Development of the enigmatic peristome of *Timmia megapolitana* (Timmiaceae; Bryophyta). *American Journal of Botany* 94: 460–467.
- Budke, J. M., N. R. Patel, G. Consortium, M. D. Wienhold, and M. A. Bruggeman-Nannenga. 2022. Exploring morphological evolution in relation to habitat moisture in the moss genus *Fissidens* using molecular data generated from herbarium specimens. *Journal of Systematics and Evolution* 61: 868–889.
- Cammarata, J., C. Morales Farfan, M. Scanlon, and A. Roeder. 2022. Cytokinin-CLAVATA cross-talk is an ancient mechanism regulating shoot meristem homeostasis in land plants. *Proceedings of the National Academy of Sciences, USA* 119: e2116860119.
- Chang, Y., and S. W. Graham. 2014. Patterns of clade support across the major lineages of moss phylogeny. *Cladistics* 30: 590–606.
- Chang, Z., G. Li, J. Liu, Y. Zhang, C. Ashby, D. Liu, C. L. Cramer, and X. Huang. 2015. Bridger: a new framework for de novo transcriptome assembly using RNA-seq data. *Genome Biology* 16: 30.
- Cooper, B. J., M. J. Moore, N. A. Douglas, W. L. Wagner, M. G. Johnson, R. P. Overson, S. P. Kinoshian, et al. 2022. Target enrichment and extensive population sampling help untangle the recent, rapid radiation of *Oenothera* sect. *Calyphus*. *Systematic Biology* 72: 249–263.
- Coudert, Y., N. Bell, C. Edelin, and C. Harrison. 2017. Multiple innovations underpinned branching form diversification in mosses. *New Phytologist* 215: 840–850.
- Coudert, Y., W. Palubicki, K. Ljung, O. Novak, O. Leyser, and C. J. Harrison. 2015. Three ancient hormonal cues co-ordinate shoot branching in a moss. *eLife* 4: 1–26.
- Cox, C. J., B. Goffinet, N. J. Wickett, S. B. Boles, and A. J. Shaw. 2010. Moss diversity: a molecular phylogenetic analysis of genera. *Phytotaxa* 9: 175–195.
- Crandall-Stotler, B. J., L. L. Forrest and R. E. Stotler. 2005. Evolutionary trends in the simple thalloid liverworts (Marchantiophyta, Jungermanniopsida subclass Metzgeriidae). *Taxon* 54: 299–316.
- Crandall-Stotler, B., and R. E. Stotler. 2000. Morphology and classification of the Marchantiophyta. In A. J. Shaw and B. Goffinet [eds.], *Bryophyte biology*, 21–70. Cambridge University Press, Cambridge, UK.
- Crandall-Stotler, B. J., R. E. Stotler, and D. G. Long. 2009a. Morphology and classification of the Marchantiophyta. In B. Goffinet and A. J. Shaw [eds.], *Bryophyte biology*, 1–54. Cambridge University Press, NY, NY, USA.
- Crandall-Stotler, B., R. E. Stotler, and D. G. Long. 2009b. Phylogeny and classification of the Marchantiophyta. *Edinburgh Journal of Botany* 66: 155–198.
- Crosby, M. R. 1980. The diversity and relationships of mosses. In R. J. Taylor and A. E. Leviton [eds.], *The mosses of North America: an inquiry into the biology of mosses based upon a symposium*, 115–129. Pacific Division of the American Association for the Advancement of Science, San Francisco, CA, USA.
- Crosby, M. R., R. E. Magill, B. Allen, and S. He. 1999. A checklist of the mosses. Missouri Botanical Garden Press, St. Louis, MO, USA.
- Crum, H. 1972. The geographic origins of the mosses of North America's eastern deciduous forest. *Journal of the Hattori Botanical Laboratory* 35: 269–298.
- Crum, H. 2001. Structural diversity of bryophytes. University of Michigan Herbarium, Ann Arbor, MI, USA.
- Davis, E. C. 2004. A molecular phylogeny of leafy liverworts (Jungermanniidae: Marchantiophyta). *Monographs in Systematic Botany from the Missouri Botanical Garden* 98: 61–86.
- Degnan, J. H., and N. A. Rosenberg. 2009. Gene tree discordance, phylogenetic inference and the multispecies coalescent. *Trends in Ecology & Evolution* 24: 332–340.
- De La Torre, A. R., Z. Li, Y. Van de Peer, and P. K. Ingvarsson. 2017. Contrasting rates of molecular evolution and patterns of selection among gymnosperms and flowering plants. *Molecular Biology and Evolution* 34: 1363–1377.
- Dong, S., S. Zhang, L. Zhang, H. Wu, B. Goffinet, and Y. Liu. 2021. Plastid genomes and phylogenomics of liverworts (Marchantiophyta): conserved genome structure but highest relative plastid substitution rate in land plants. *Molecular Phylogenetics and Evolution* 161: 107171.
- Dong, S., J. Yu, L. Zhang, B. Goffinet, and Y. Liu. 2022b. Phylotranscriptomics of liverworts: revisiting the backbone phylogeny and ancestral gene duplications. *Annals of Botany* 130: 951–964.
- Dong, S.-S., H. L. Li, B. Goffinet, and Y. Liu. 2022a. Exploring the impact of RNA editing on mitochondrial phylogenetic analyses in liverworts, an early land plant lineage. *Journal of Systematics and Evolution* 60: 16–22.
- Doyle, J., and J. Doyle. 1987. A rapid DNA isolation procedure for small quantities of fresh leaf tissue. *Phytochemical Bulletin* 19: 11–15.
- Draper, I., T. Villaverde, R. Garilleti, J. G. Burleigh, S. F. McDaniel, V. Mazimpaka, J. A. Calleja, and F. Lara. 2022. An NGS-based phylogeny of Orthotrichaceae (Orthotrichaceae, Bryophyta) with the proposal of the new genus *Rehubyrum* from Zealandia. *Frontiers in Plant Science* 13: 882960.
- Duff, J., J. C. Villarreal, C. Cargill, and K. Renzaglia. 2007. Progress and challenges toward developing a phylogeny and classification of the hornworts. *Bryologist* 110: 214–243.
- Duff, R. J., D. C. Cargill, J. C. Villarreal, and K. S. Renzaglia. 2004. Phylogenetic relationships of the hornworts based on *rbcL* sequence data: novel relationships and new insights. *Annals of the Missouri Botanical Gardens* 98: 41–58.
- Eldridge, D. J., E. Guirado, P. B. Reich, R. Ochoa-Hueso, M. Berdugo, T. Sáez-Sandino, J. L. Blanco-Pastor, et al. 2023. The global contribution of soil mosses to ecosystem services. *Nature Geoscience* 16: 430–438.
- Fedosov, V. E., A. V. Fedorova, A. E. Fedosov, and M. S. Ignatov. 2016. Phylogenetic inference and peristome evolution in haplolepidous mosses, focusing on Pseudoditrichaceae and Ditrichaceae s. l. *Botanical Journal of the Linnean Society* 181: 139–155.
- Fedosov, V., A. Fedorova, E. Ignatova, and J. Kučera. 2023. New taxonomic arrangement of *Dicranella* s.l. and *Aongstroemia* s.l. (Dicranidae, Bryophyta). *Plants* 12: 1360.
- Fedosov, V. E., A. V. Fedorova, J. Larraín, M. B. Santos, M. Stech, J. Kučera, J. C. Brinda, et al. 2021. Unity in diversity: phylogenetics and taxonomy of Rhabdoweisiaceae (Dicranales, Bryophyta). *Botanical Journal of the Linnean Society* 195: 545–567.
- Feldberg, K., S. R. Gradstein, C. Gröhn, J. Heinrichs †, M. Von Konrat, Y. S. Mamontov, M. A. M. Renner, et al. 2021. Checklist of fossil liverworts suitable for calibrating phylogenetic reconstructions. *Bryophyte Diversity and Evolution* 43: 14–71.
- Feldberg, K., H. Schneider, T. Stadler, A. Schäfer-Verwimp, A. Schmidt, and J. Heinrichs. 2014. Epiphytic leafy liverworts diversified in angiosperm-dominated forests. *Scientific Reports* 4: 5974.
- Fife, A. J., and P. J. Dalton. 2005. A reconsideration of *Pleurophascum* (Musci: Pleurophascaceae) and specific status for a New Zealand endemic, *Pleurophascum ovalifolium* stat. et nom. nov. *New Zealand Journal of Botany* 43: 871–884.
- Forrest, L. L., E. C. Davis, D. G. Long, B. J. Crandall-Stotler, A. Clark, and M. L. Hollingsworth. 2006. Unraveling the evolutionary history of the liverworts (Marchantiophyta): multiple taxa, genomes and analyses. *Bryologist* 109: 303–334.
- Frey, W., and M. Stech. 2005. A morpho-molecular classification of the liverworts (Hepaticophytina, Bryophyta). *Nova Hedwigia* 81: 55–78.

- Glime, J. M. 1990. Primitive or advanced? *Bryological Times* 55: 5–7.
- Goffinet, B. 1997. The Rhachithecaceae: revised circumscription and ordinal affinities. *The Bryologist* 100: 425–439.
- Goffinet, B., R. J. Bayer, and D. H. Vitt. 1998. Circumscription and phylogeny of the Orthotrichales (Bryopsida) inferred from *rbcl* sequence analysis. *American Journal of Botany* 85: 1324–1337.
- Goffinet, B., and W. R. Buck. 2004. Systematics of Bryophyta: from molecules to a revised classification. *Monographs in Systematic Botany from the Missouri Botanical Garden* 98: 205–239.
- Goffinet, B., W. Buck, and J. Shaw. 2009a. Addenda to the classification of mosses. I. Andreaephytina stat. nov. and Andreaebryophytina stat. nov. *The Bryologist* 112: 856–857.
- Goffinet, B., W. Buck, and J. Shaw. 2009b. Morphology, anatomy, and classification of the Bryophyta. In B. Goffinet and A. J. Shaw [eds.], *Bryophyte biology*, 55–138. Cambridge University Press, NY, USA.
- Goffinet, B., C. J. Cox, A. J. Shaw, and T. A. Hedderson. 2001. The Bryophyta (mosses): systematic and evolutionary inferences from an *rps4* gene (cpDNA) phylogeny. *Annals of Botany* 87: 191–208.
- Harris, B. J., J. W. Clark, D. Schrempf, G. J. Szöllösi, P. C. J. Donoghue, A. M. Hetherington, and T. A. Williams. 2022. Divergent evolutionary trajectories of bryophytes and tracheophytes from a complex common ancestor of land plants. *Nature Ecology & Evolution* 6: 1634–1643.
- Harris, B. J., C. J. Harrison, A. M. Hetherington, and T. A. Williams. 2020. Phylogenomic evidence for the monophyly of bryophytes and the reductive evolution of stomata. *Current Biology* 30: 1–12.
- Hässel de Menéndez, G. G. 1988. A proposal for a new classification of the genera within the Anthocerotophyta. *Journal of the Hattori Botanical Laboratory* 64: 71–86.
- He-Nygrén, X., I. Ahonen, A. Juslén, D. Glenny, and S. Piippo. 2004. Phylogeny of liverworts-beyond a leaf and a thallus. *Monographs in Systematic Botany from the Missouri Botanical Garden* 98: 87–118.
- Hedderson, T. A., C. J. Cox, and J. G. Gibbins. 1999. Phylogenetic relationships of the Wardiaceae (Musci); evidence from 18S rRNA and *rps4* gene sequences. *Bryologist* 102: 26–31.
- Hedderson, T. A., D. J. Murray, C. J. Cox, and T. L. Nowell. 2004. Phylogenetic relationships of haplolepidous mosses (Dicranidae) inferred from *rps4* gene sequences. *Systematic Botany* 29: 29–41.
- Heinrichs, J., S. R. Gradstein, R. Wilson, and H. Schneider. 2005. Towards a natural classification of liverworts (Marchantiophyta) based on the chloroplast gene *rbcl*. *Cryptogamie, Bryologie* 26: 131–150.
- Hoang, D. T., O. Chernomor, A. von Haeseler, B. Q. Minh, and L. Vinh. 2017. UFBoot2: Improving the ultrafast bootstrap approximation. *Molecular Biology and Evolution* 35: 518–522.
- Huttunen, S., N. Bell, and L. Hedenäs. 2018. The evolutionary diversity of mosses – taxonomic heterogeneity and its ecological drivers. *Critical Reviews in Plant Sciences* 37: 128–174.
- Huttunen, S., and M. S. Ignatov. 2010. Evolution and taxonomy of aquatic species in the genus *Rhynchostegium* (Brachytheciaceae, Bryophyta). *Taxon* 59: 791–808.
- Hyvönen, J., and S. Piippo. 1993. Cladistic analysis of the hornworts (Anthocerotophyta). *Journal of the Hattori Botanical Laboratory* 74: 105–119.
- Ignatov, M. S., and E. V. Maslova. 2021. Fossil mosses: What do they tell us about moss evolution? *Bryophyte Diversity and Evolution* 43: 72–97.
- Ignatov, M. S., U. N. Spirina, M. A. Kolesnikova, L. F. Volosnova, S. V. Polevova, and E. A. Ignatova. 2018. *Buxbaumia*: a moss peristome without a peristomial formula. *Arctoa* 27: 172–202.
- Ingold, C. T. 1959. Peristome teeth and spore discharge in mosses. *Transactions of the Botanical Society of Edinburgh* 38: 76–88.
- Jauregui-Lazo, J., J. C. Brinda, and B. D. Mishler. 2023. The phylogeny of *Syntrichia*: an ecologically diverse clade of mosses with an origin in South America. *American Journal of Botany* 110: e16103.
- Junier, T., and E. M. Zdobnov. 2010. The Newick utilities: high-throughput phylogenetic tree processing in the Unix shell. *Bioinformatics* 26: 1669–1670.
- Laenen, B., B. Shaw, H. Schneider, B. Goffinet, E. Paradis, A. Désamoré, J. Heinrichs, et al. 2014. Extant diversity of bryophytes emerged from successive post-Mesozoic diversification bursts. *Nature Communications* 5: 5134.
- La Farge, C., B. D. Mishler, J. A. Wheeler, D. P. Wall, K. Johannes, S. Schaffer, and A. J. Shaw. 2000. Phylogenetic relationships within the haplolepidous mosses. *Bryologist* 103: 257–276.
- La Farge-England, C. 1996. Growth form, branching pattern, and perichaetial position in mosses: cladocarp and pleurocarpy redefined. *Bryologist* 99: 170.
- Larsson, A. 2014. AliView: a fast and lightweight alignment viewer and editor for large datasets. *Bioinformatics* 30: 3276–3278.
- Lavy, M., M. Prigge, S. Tao, S. Shain, A. Kuo, K. Kirchsteiger, and M. Estelle. 2016. Constitutive auxin response in *Physcomitrella* reveals complex interactions between Aux/IAA and ARF proteins. *eLife* 5: 1–22.
- Leebens-Mack, J., M. Barker, E. Carpenter, M. Deyholos, M. Gitzendanner, S. Graham, I. Grosse, et al. 2019. One thousand plant transcriptomes and the phylogenomics of green plants. *Nature* 574: 679–685.
- Liaimer, A., J. Jensen, and E. Dittmann. 2016. A genetic and chemical perspective on symbiotic recruitment of cyanobacteria of the genus *Nostoc* into the host plant *Blasia pusilla* L. *Frontiers in Microbiology* 7: 1–16.
- Lin, S. H. 1983. A taxonomic revision of Phyllogoniaceae (Bryopsida). Part I. *Journal of the Taiwan Museum* 36: 37–86.
- Liu, Y., M. Johnson, C. Cox, R. Medina, N. Devos, A. Vanderpoorten, L. Hedenäs, et al. 2019. Resolution of the ordinal phylogeny of mosses using targeted exons from organellar and nuclear genomes. *Nature Communications* 10: 1–11.
- Lloyd, G. T., K. E. Davis, D. Pisani, J. E. Tarver, M. Ruta, M. Sakamoto, D. W. E. Hone, et al. 2008. Dinosaurs and the Cretaceous terrestrial revolution. *Proceedings of the Royal Society, B, Biological Sciences* 275: 2483–2490.
- Lovis, J. D. 1977. Evolutionary patterns and processes in ferns. In R. D. Preston and H. W. Woolhouse [eds.], *Advances in botanical research*, 229–440. Academic Press, London, UK.
- Lücking, R. 2019. Stop the abuse of time! Strict temporal banding is not the future of rank-based classifications in fungi (including lichens) and other organisms. *Critical Reviews in Plant Sciences* 38: 199–253.
- Magill, R. E. 1977. Towards the conservation of four family names in Musci. *Taxon* 26: 597–598.
- Maurin, K. J. L. 2020. An empirical guide for producing a dated phylogeny with treePL in a maximum likelihood framework. *arXiv*. 2008: 07054.
- McCourt, R. M., L. A. Lewis, P. K. Strother, C. F. Delwiche, N. J. Wickett, J. de Vries, and J. L. Bowman. 2023. Green land: Multiple perspectives on green algal evolution and the earliest land plants. *American Journal of Botany* 110: e16175.
- Meagher, D., A. Cairns, R. Seppelt, and M. Grixti. 2020. A re-evaluation of the morphology of *Sorapilla* (Bryophyta: Sorapillaceae) based on *Sorapilla papuana*. *Australian Systematic Botany* 33: 427–435.
- Medina, R., M. G. Johnson, Y. Liu, N. J. Wickett, A. J. Shaw, and B. Goffinet. 2019. Phylogenomic delineation of *Physcomitrium* (Bryophyta: Funariaceae) based on targeted sequencing of nuclear exons and their flanking regions rejects the retention of *Physcomitrella*, *Physcomitridium* and *Aphanorrhagma*. *Journal of Systematics and Evolution* 57: 404–417.
- Miller, M., W. Pfeiffer, and T. Schwartz. 2011. The CIPRES science gateway. Proceedings of the 2011 TeraGrid Conference: Extreme digital discovery, 1–8. ACM, NY, NY, USA.
- Minh, B. Q., M. W. Hahn, and R. Lanfear. 2020. New methods to calculate concordance factors for phylogenomic datasets. *Molecular Biology and Evolution* 37: 2727–2733.
- Morales-Briones, D., G. Kadereit, D. Tefarikis, M. Moore, S. Smith, S. Brockington, A. Timoneda, et al. 2021. Disentangling sources of gene tree discordance in phylogenomic data sets: testing ancient hybridizations in Amaranthaceae s.l. *Systematic Biology* 70: 219–235.
- Morris, J. L., M. N. Puttick, J. W. Clark, D. Edwards, P. Kenrick, S. Pressel, C. H. Wellman, et al. 2018. The timescale of early land plant evolution. *Proceedings of the National Academy of Sciences, USA* 115: E2274–E2283.
- Newton, A. E., N. Wikström, N. Bell, L. L. Forrest, and M. S. Ignatov. 2007. Dating the diversification of the pleurocarpous mosses. *Systematic Association Special Volume* 71: 41–64.

- Nguyen, L.-T., H. Schmidt, A. von Haeseler, and B. Q. Minh. 2015. IQ-TREE: a fast and effective stochastic algorithm for estimating maximum-likelihood phylogenies. *Molecular Biology and Evolution* 32: 268–274.
- Paradis, E., and K. Schliep. 2019. ape 5.0: an environment for modern phylogenetics and evolutionary analyses in R. *Bioinformatics* 35: 526–528.
- Patiño, J., I. Bisang, B. Goffinet, L. Hedenäs, S. McDaniel, S. Pressel, M. Stech, et al. 2022. Unveiling the nature of a miniature world: a horizon scan of fundamental questions in bryology. *Journal of Bryology* 44: 1–34.
- Porada, P., B. Weber, W. Elbert, U. Pöschl, and A. Kleidon. 2013. Estimating global carbon uptake by lichens and bryophytes with a process-based model. *Biogeosciences* 10: 6989–7033.
- Porada, P., B. Weber, W. Elbert, U. Pöschl, and A. Kleidon. 2014. Estimating impacts of lichens and bryophytes on global biogeochemical cycles. *Global Biogeochemical Cycles* 28: 71–85.
- Pursell, R. A. 2017. A taxonomic revision of the Erpodiaceae (Bryophyta). *Memoirs of the New York Botanical Garden* 116: 1–105.
- Puttick, M., J. Morris, T. Williams, C. Cox, D. Edwards, P. Kenrick, S. Pressel, et al. 2018. The interrelationships of land plants and the nature of the ancestral embryophyte. *Current Biology* 28: 733–745.e2.
- R Core Team, R. 2020. R: a language and environment for statistical computing. Foundation for Statistical Computing, Vienna, Austria. Website: <https://www.r-project.org/>
- Rambaut, A. 2017. FigTree-version 1.4. 3, a graphical viewer of phylogenetic trees. Website: <http://tree.bio.ed.ac.uk/software/figtree/> [accessed 20 August 2018].
- Rensing, S. A., B. Goffinet, R. Meyberg, S.-Z. Wu, and M. Bezanilla. 2020. The moss *Physcomitrium* (*Physcomitrella*) *patens*: a model organism for non-seed plants. *Plant Cell* 32: 1361–1376.
- Renzaglia, K. S., and J. G. Duckett. 1987. Spermatogenesis in *Blasia pusilla*: from young antheridium through mature spermatozoid. *Bryologist* 90: 419.
- Renzaglia, K. S., J. C. Villarreal, and R. J. Duff. 2009. New insights into morphology, anatomy, and systematics of hornworts. In B. Goffinet and A. J. Shaw [eds.], *Bryophyte biology*, 139–171. Cambridge University Press, NY, NY, USA.
- Renzaglia, K. S., J. C. Villarreal A., and D. J. Gabary. 2018. Morphology supports the setaphyte hypothesis: mosses plus liverworts form a natural group. *Bryophyte Diversity and Evolution* 40: 11–17.
- Rich, M., and P.-M. Delaux. 2020. Plant evolution: when *Arabidopsis* is more ancestral than *Marchantia*. *Current Biology* 30: R642–R644.
- Sanderson, M. J. 2003. r8s: inferring absolute rates of molecular evolution and divergence times in the absence of a molecular clock. *Bioinformatics* 19: 301–302.
- Sawangproh, W., A. S. Lang, L. Hedenäs, and N. Cronberg. 2020. Morphological characters and SNP markers suggest hybridization and introgression in sympatric populations of the pleurocarpus mosses *Homalothecium lutescens* and *H. sericeum*. *Organisms Diversity & Evolution* 20: 619–637.
- Sayyari, E., and S. Mirarab. 2016. Fast coalescent-based computation of local branch support from quartet frequencies. *Molecular Biology and Evolution* 33: 1654–1668.
- Schljakov, R. N. 1972. On the higher taxa of liverworts—class Hepaticae s. str. *Botanicheskii Zhurnal* 57: 496–508.
- Schuettpelz, E., and K. M. Pryer. 2009. Evidence for a Cenozoic radiation of ferns in an angiosperm-dominated canopy. *Proceedings of the National Academy of Sciences, USA* 106: 11200–11205.
- Schuster, R. M. 1984. Evolution, phylogeny and classification of the Hepaticae. In R. M. Schuster [ed.], *New manual of bryology*, vol. 2, 892–1070. Hattori Botanical Laboratory, Nichinan, Japan.
- Schuster, R. M. 1992. The Hepaticae and Anthocerotae of North America, vol. VI. Field Museum of Natural History, Chicago, IL, USA.
- Shaw, A. J., L. E. Anderson, and B. D. Mishler. 1987. Peristome development in mosses in relation to systematics and evolution. I. *Diphysium foliosum* (Buxbaumiacae). *Memoirs of the New York Botanical Garden* 45: 55–70.
- Shaw, A. J., C. Cox, B. Goffinet, W. Buck, and S. Boles. 2003. Phylogenetic evidence of a rapid radiation of pleurocarpus mosses (Bryophyta). *Evolution* 57: 2226–2241.
- Shaw, B., B. Crandall-Stotler, J. Vána, R. E. Stotler, M. von Konrat, J. J. Engel, E. C. Davis, et al. 2015. Phylogenetic relationships and morphological evolution in a major clade of leafy liverworts (phylum Marchantiophyta, order Jungermanniales): suborder Jungermanniineae. *Systematic Botany* 40: 27–45.
- Smith, S., and B. O'Meara. 2012. treePL: divergence time estimation using penalized likelihood for large phylogenies. *Bioinformatics* 28: 2689–2690.
- Söderström, L., A. Hagborg, M. von Konrat, S. Bartholomew-Began, D. Bell, L. Briscoe, E. Brown, et al. 2016. World checklist of hornworts and liverworts. *PhytoKeys* 59: 1–828.
- Sousa, F., P. Foster, P. Donoghue, H. Schneider, and C. Cox. 2019. Nuclear protein phylogenies support the monophyly of the three bryophyte groups (Bryophyta Schimp.). *New Phytologist* 222: 565–575.
- Spitale, D., and A. Petraglia. 2010. *Palustriella falcata* (Brid.) Hedenäs (Amblystegiaceae, Bryopsida) with pluristratose lamina: morphological variability of specimens in springs of the Italian Alps. *Plant Systematics and Evolution* 286: 59–68.
- Stamatakis, A. 2006. RAXML-VI-HPC: maximum likelihood-based phylogenetic analyses with thousands of taxa and mixed models. *Bioinformatics* 22: 2688–2690.
- Stech, M., and W. Frey. 2008. A morpho-molecular classification of the mosses (Bryophyta). *Nova Hedwigia* 86: 1–21.
- Stech, M., S. F. McDaniel, R. Hernández-Maqueda, R. M. Ros, O. Werner, J. Muñoz, and D. Quandt. 2012. Phylogeny of haplolepidous mosses—challenges and perspectives. *Journal of Bryology* 34: 173–186.
- Stamatakis, A. 2014. RAXML version 8: a tool for phylogenetic analysis and post-analysis of large phylogenies. *Bioinformatics* 30: 1312–1313.
- Stotler, R. E., and B. Crandall-Stotler. 2005. A revised classification of the Anthocerotophyta and a checklist of the hornworts of North America, north of Mexico. *Bryologist* 108: 16–26.
- Stuart, J., H. Holland-Moritz, L. Lewis, M. Jean, S. Miller, S. McDaniel, N. Fierer, et al. 2021. Host identity as a driver of moss-associated N₂ fixation rates in Alaska. *Ecosystems* 24: 530–547.
- Stull, G. W., K. K. Pham, P. S. Soltis, and D. E. Soltis. 2023. Deep reticulation: the long legacy of hybridization in vascular plant evolution. *Plant Journal* 114: 743–766.
- Tomescu, A. M. F., B. Bomfleur, A. C. Bippus, and M. A. Savoretti. 2018. Why are bryophytes so rare in the fossil record? A focus on taphonomy and fossil preservation. In M. Krings, C. J. Harper, N. R. Cúneo, and G. W. Rothwell [eds.], *Transformative paleobotany: papers to commemorate the life and legacy of Thomas N. Taylor*, 375–415. Academic Press, San Francisco, CA, USA.
- Villarreal, J. C., B. Crandall-Stotler, M. Hart, D. Long, and L. Forrest. 2016. Divergence times and the evolution of morphological complexity in an early land plant lineage (Marchantiopsida) with a slow molecular rate. *New Phytologist* 209: 1734–1746.
- Villarreal, J. C., N. Cusimano, and S. Renner. 2015. Biogeography and diversification rates in hornworts: The limitations of diversification modeling. *Taxon* 64: 229–238.
- Villarreal, J. C., and S. Renner. 2012. Hornwort pyrenoids, carbon-concentrating structures, evolved and were lost at least five times during the last 100 million years. *Proceedings of the National Academy of Sciences, USA* 109: 18873–18878.
- Vitt, D. H. 1981. Adaptive modes of the moss sporophyte. *Bryologist* 84: 166–186.
- Vitt, D. H. 1982. Bryopsida. In S. P. Parker [ed.], *Synopsis and classification of living organisms*, vol. 1, 307–336. McGraw-Hill, NY, NY, USA.
- Vitt, D. H. 1984. Classification of the Bryopsida. In R. M. Schuster [ed.], *New manual of bryology*, vol. 2, 696–759. Hattori Botanical Laboratory, Nichinan, Japan.
- Vitt, D. H. 1995. The genus *Calomnion* (Bryopsida): taxonomy, phylogeny, and biogeography. *Bryologist* 98: 338–358.
- Wu, M., J. L. Kostyun, M. W. Hahn, and L. C. Moyle. 2018. Dissecting the basis of novel trait evolution in a radiation with widespread phylogenetic discordance. *Molecular Ecology* 27: 3301–3316.
- Yu, Y., J. B. Yang, W. Z. Ma, S. Pressel, H. M. Liu, Y. H. Wu, and H. Schneider. 2020. Chloroplast phylogenomics of liverworts: a

reappraisal of the backbone phylogeny of liverworts with emphasis on Ptilidiales. *Cladistics* 36: 184–193.

Zhang, C., M. Rabiee, E. Sayyari, and S. Mirarab. 2018. ASTRAL-III: polynomial time species tree reconstruction from partially resolved gene trees. *BMC Bioinformatics* 19: 153.

SUPPORTING INFORMATION

Additional supporting information can be found online in the Supporting Information section at the end of this article.

APPENDIX S1. Tables S1–12.

APPENDIX S2. Annotated ASTRAL phylogeny of hornworts inferred from nucleotide data, highlighting (supra-) ordinal relationships.

APPENDIX S3. Annotated ASTRAL phylogeny of liverworts inferred from nucleotide data, highlighting suprafamilial relationships.

APPENDIX S4. Annotated ASTRAL phylogeny of mosses inferred from nucleotide data, highlighting suprafamilial relationships.

APPENDIX S5. Annotated ASTRAL phylogeny of hornworts inferred from amino acid data, highlighting (supra-) ordinal relationships.

APPENDIX S6. Annotated ASTRAL phylogeny of liverworts inferred from amino acid data, highlighting suprafamilial relationships.

APPENDIX S7. Annotated ASTRAL phylogeny of mosses inferred from amino acid data, highlighting suprafamilial relationships.

APPENDIX S8. Divergence times estimates for bryophytes inferred by penalized likelihood using 29 fossil calibrations.

APPENDIX S9. Correlation between gene concordance factor inferred by IQ-TREE and number of genes in the nucleotide dataset supporting a node.

APPENDIX S10. Correlation between gene concordance factor inferred by IQ-TREE and mean divergence times for backbone nodes (between 130 and 450 Ma) inferred from the nucleotide data.

APPENDIX S11. Histogram of the frequency of estimated (A) stem and (B) crown age divergences for orders and families of three bryophyte phyla (Anthocerotophyta, Bryophyta, and Marchantiophyta).

APPENDIX S12. Histogram of the frequency of estimated crown ages for orders and families of the three bryophyte phyla (Anthocerotophyta, Bryophyta, and Marchantiophyta).

How to cite this article: Bechteler, J., G. Peñaloza-Bojacá, D. Bell, J. G. Burleigh, S. F. McDaniel, E. C. Davis, E. B. Sessa, et al. 2023. Comprehensive phylogenomic time tree of bryophytes reveals deep relationships and uncovers gene incongruences in the last 500 million years of diversification. *American Journal of Botany* 110(11): e16249.
<https://doi.org/10.1002/ajb2.16249>